

Accepted Manuscript

Synthesis, biological evaluation, and molecular docking study of sulfonate derivatives as nucleotide pyrophosphatase (NPPs) inhibitors

Mohammad H. Semreen, Mohammed I. El-Gamal, Saif Ullah, Saquib Jalil, Sumera Zaib, Hanan S. Anbar, Joanna Lecka, Jean Sévigny, Jamshed Iqbal

PII: S0968-0896(19)30571-1
DOI: <https://doi.org/10.1016/j.bmc.2019.04.031>
Reference: BMC 14885

To appear in: *Bioorganic & Medicinal Chemistry*

Received Date: 8 April 2019
Revised Date: 23 April 2019
Accepted Date: 25 April 2019

Please cite this article as: Semreen, M.H., El-Gamal, M.I., Ullah, S., Jalil, S., Zaib, S., Anbar, H.S., Lecka, J., Sévigny, J., Iqbal, J., Synthesis, biological evaluation, and molecular docking study of sulfonate derivatives as nucleotide pyrophosphatase (NPPs) inhibitors, *Bioorganic & Medicinal Chemistry* (2019), doi: <https://doi.org/10.1016/j.bmc.2019.04.031>

This is a PDF file of an unedited manuscript that has been accepted for publication. As a service to our customers we are providing this early version of the manuscript. The manuscript will undergo copyediting, typesetting, and review of the resulting proof before it is published in its final form. Please note that during the production process errors may be discovered which could affect the content, and all legal disclaimers that apply to the journal pertain.



Synthesis, biological evaluation, and molecular docking study of sulfonate derivatives as nucleotide pyrophosphatase (NPPs) inhibitors

Mohammad H. Semreen^{1,2}, Mohammed I. El-Gamal^{1,2,3,*}, Saif Ullah⁴, Saqib Jalil⁴, Sumera Zaib⁴, Hanan S. Anbar³, Joanna Lecka^{5,6}, Jean Sévigny^{5,6}, and Jamshed Iqbal^{4,*}

¹ Department of Medicinal Chemistry, College of Pharmacy, University of Sharjah, Sharjah 27272, United Arab Emirates.

² Sharjah Institute for Medical Research, University of Sharjah, Sharjah 27272, United Arab Emirates.

³ Faculty of Pharmacy, University of Mansoura, Mansoura 35516, Egypt.

⁴ Centre for Advanced Drug Research, COMSATS University Islamabad, Abbottabad Campus, Abbottabad-22060, Pakistan.

⁵ Département de microbiologie-infectiologie et d'immunologie, Faculté de Médecine, Université Laval, Québec, QC, G1V 0A6, Canada.

⁶ Centre de Recherche du CHU de Québec – Université Laval, Québec, QC, G1V 4G2, Canada.

***Corresponding authors:** e-mail address: drmelgamal2002@gmail.com ; address: Department of Medicinal Chemistry, College of Pharmacy, University of Sharjah, Sharjah 27272, United Arab Emirates [M.I. El-Gamal] & e-mail address: drjamshed@cuiatd.edu.pk; address: Centre for Advanced Drug Research, COMSATS University Islamabad, Abbottabad Campus, Abbottabad-22060, Pakistan [J. Iqbal].

Abstract

A new series of sulfonate derivatives **1a-zk** were synthesized and evaluated as inhibitors of nucleotide pyrophosphatases. Most of the compounds exhibited good to moderate inhibition towards NPP1, NPP2, and NPP3 isozymes. Compound **1m** was a potent and selective inhibitor of NPP1 with an IC_{50} value of $0.387 \pm 0.007 \mu\text{M}$. However, the most potent inhibitor of NPP3 was found as **1x** with an IC_{50} value of $0.214 \pm 0.012 \mu\text{M}$. In addition, compound **1e** was the most active inhibitor of NPP2 with an IC_{50} value of $0.659 \pm 0.007 \mu\text{M}$. Docking studies of the most potent compounds were carried out, and the computational results supported the *in vitro* results.

Keywords: Homology modeling; Immune modulation; Molecular docking; Nucleotide pyrophosphatase; Sulfonate.

1. Introduction

Cells communicate via a route of purinergic signaling that is arbitrated by a number of extracellularly positioned nucleotides accompanying nucleosides. This purine nucleotide and nucleoside signaling play a role in the synaptic transmission, determination of cell fate, and immunologic response. Secreted nucleotides are capable of switching receptors on cell surface named P1, P2X and P2Y.¹ A number of extracellular nucleotide-hydrolyzing enzyme classes are engaged in terminating purinergic signaling. The classes of cell surface-located proteins include ecto-nucleoside triphosphate diphosphohydrolases (ENTPDases), alkaline phosphatases (APs), and the ectonucleotide pyrophosphatases/phosphodiesterases (ENPPs).² ENPPs deal with multiple nucleotide substrates, in particular nucleotide triphosphate, nucleotide diphosphates, nucleotide sugars, and dinucleotide polyphosphates to generate nucleotide monophosphate (NMP) as product. NMP is hydrolyzed by APs and ecto-5'-nucleotidases (eNs) and release nucleoside as a final product.¹⁻³

In accordance with relation to substrate preference, seven members of human ENPPs can be grouped into two categories. ENPP1, 3, 4 occupy first category for nucleotide degrading potency, and second category may include ENPP2, 6, 7 which have affinity for phospholipid-

based substrates. ENPP1 early represented as PC1, is a homodimer (linked with disulfide bonds) glycoprotein.⁴ Inorganic pyrophosphate generated as a result of nucleotide hydrolysis by ENPP1, selectively binds to hydroxyapatite crystals and inhibits the bone mineralization.⁵ In contrast to PPi, produced by tissue non-specific alkaline phosphatase (TNAP), which facilitates the bone formation.^{6,7} Reduced level of ENPP1 is associated with atherosclerosis,⁸ hypophosphatemic rickets⁹ and general arterial calcification of infancy (GACI).¹⁰ On the other hand, over expression of ENPP1 leads to the release of calcium pyrophosphate dihydrate (CPPD) that accumulate in the joints resulting in disorder chondrocalcinosis.¹¹ Increased level of PPi causes chondrocytes apoptosis, facilitating the disorder osteoarthritis¹² and aortic valve calcification.¹³

ENPP2 is a distinctive among the other members, capable of producing lysophosphatidic acids (LPA), in particular from lysophosphatidylcholine (LPC),¹⁴ by hydrolyzing the phosphodiester bonds of substrate. Non-nucleotide substrates for ENPP2 include lipid compounds and phosphate esters of choline, however, it has also affinity for nucleotide substrates to some extent. The crystallographic structure of ENPP2 is much related in sequence identity (about 45%) to ENPP1, in which catalytic domain phosphodiesterase (PDE) is surrounded at *N*-terminal by somatomedin B-like domain and nuclease like domain via *C*-terminal.¹⁵ ENPP2 crystal structure^{16,17} also revealed a rigid hydrophobic pocket capable for binding of acyl chain of lysophospholipid, whereas deep hydrophilic region coordinate the glycerol moiety of lysophospholipid and nucleotide substrate as well. The *N*-terminal of hydrophobic pocket acts like a signal peptide, explaining the statement that ENPP2 is a secreted protein.¹⁸ The somatomedin B (SMB)-like domains in contact with catalytic region contribute to the genesis of open tunnel for LPA product, transport it to its associated G protein coupled receptors¹⁹ and binds the ENPP2 with the integrin's on cell surface as well.^{20,21} Different signaling pathways are activated by ENPP2 (autotaxin) and formed LPA product that leads to invigoration of cell survival, proliferation and migration.²² Pathophysiological contribution of LPA is reported in a number of illness including cancer,²³ fibrotic upset (pulmonary fibrosis),²⁴ neuropathic pain,²⁵ inflammatory affliction,²⁶ as well as cardiovascular²⁷ and cholestatic pruritus.²⁸

ENPP3 (CD203c) is expressed in different body organs²⁹ on surfaces such as epithelial, mucosal,³⁰ especially on mast cells and basophils.³¹ The crystal structure of ENPP3 revealed the

presence of parallel β -sheets based eight stranded catalytic phosphodiesterase (PDE) region holding five active *N*-glycosylation places and on each side, eight α -helices, representing a characteristic feature of alkaline phosphatase superfamily.^{32,33} This PDE domain is connected to nuclease-like (NUC) region via a linker L2, two somatomedin B like domains SMB1 and SMB2, attached to NUC with linker L1.³⁴ Catalytic regions occupy two zinc ions (Zn1 and Zn2) surrounded by seven amino acids side chains. Zn1 is linked by Asp-325, His-483, and His-329, and facilitates the escape of leaving group, whereas Zn2 allows nucleophilic attacks coordinated by Asp-167, Asp 372, His-373, and nucleophilic residue Thr-205.³⁵ Upregulation of ENPP3 was reported on cell surface in addition to other inflammatory mediators as a result basophils activation with antigen bounded IgE.³⁶ As a response to this activation, ATP releases which is degraded by ENPP3, thus, ENPP3 act as a marker for recognizing allergen responsiveness on basophils of patients.³⁷ In rats, this enzyme was reported in intestine possibly facilitating the absorption and digestion of nucleotides in diet.³⁸ ENPP3 is actively engaged in fluid homeostasis, modulating bile formation and secretions of cerebral spinal fluid.³⁹ ENPP3 is incriminated in synchronizing the glycosylation of nucleotide sugars of brain specific proteins⁴⁰ and hydrolyzing the intracellular and extracellular dipolyphosphate.^{41,42} Thus the involvement of these three isozymes in various biological and pathophysiological processes made them attractive target for development of therapeutic leads. Up to now, very few inhibitors of ENPP1, 3 have been identified (Fig. 1) with different potential nucleus. These compounds are non-selective, unstable and not easy to synthesize due to bulk structure. Whereas, in case of ENPP2, large number of lipid based compounds were reported, capable of targeting lysophospholipase D activity but a very small number of compounds were available against phosphodiesterase inhibition (Fig. 1). Here, we developed a new class of sulfonate derivatives and evaluated their phosphodiesterase inhibitory potential against all the three isozymes.

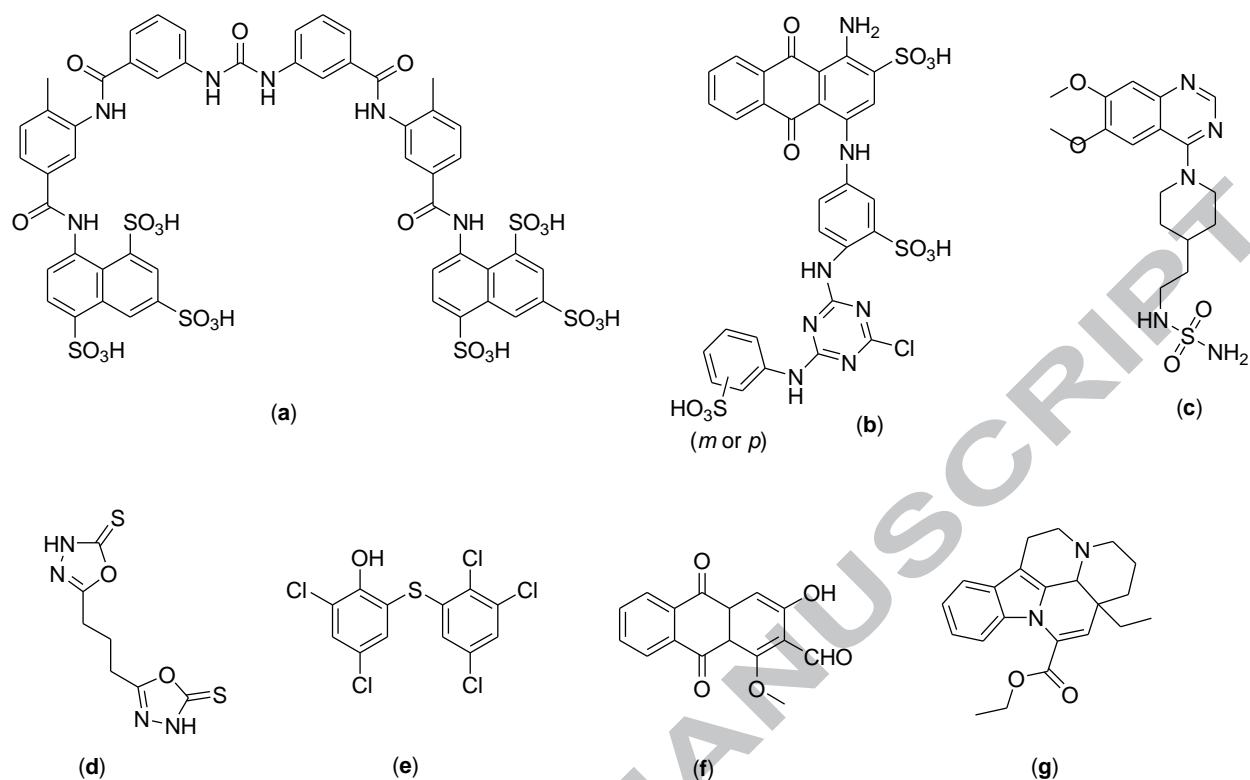


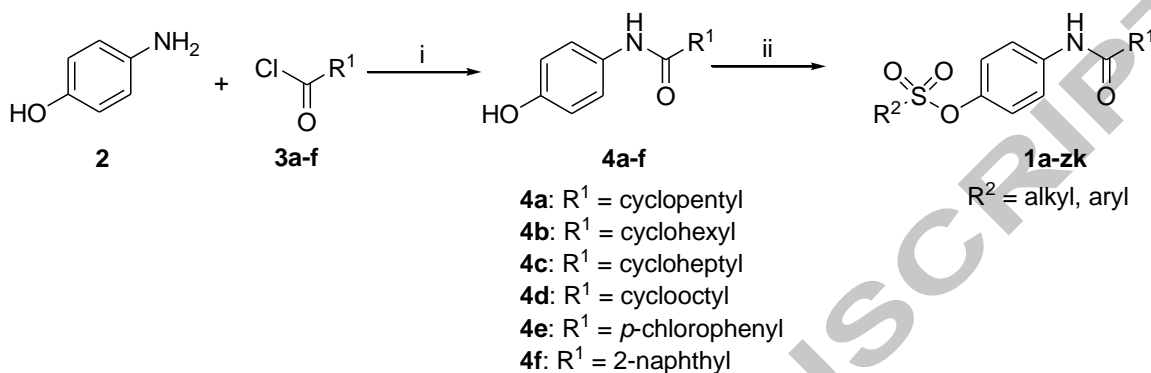
Figure 1. Structures of previously published NPP1 inhibitors. (a) Suramin,⁴³ (b) Reactive blue 2,⁴³ (c) Quinazoline-4-piperidine-4-ethylsulfamide derivative,⁴⁴ (d) Oxadiazole derivative. Non-lipid NPP2 inhibitors⁴⁵⁻⁴⁷ (e) Hexachlorophene, (f) Damnacanthal (g) Vinpocetine.

2. Results and discussion

2.1. Chemistry

The target sulfonate compounds **1a-zk** were synthesized through the 2-step synthetic pathway illustrated in Scheme 1. Reaction of *p*-aminophenol (**2**) with the appropriate acid chloride **3a-f** to produce the corresponding phenolic intermediates **4a-f**. In order to keep the hydroxyl group free and avoid diacylation, the acid chloride was diluted in acetone and added dropwise slowly to a mixture of 4-aminophenol and potassium carbonate in acetone while stirring. The target sulfonate derivatives **1a-zk** were obtained through treatment of the phenolic intermediates **4a-f** with the appropriate sulfonyl chloride reagent in presence of

triethylamine. The target compounds were purified by column chromatography and their identity and purity were confirmed by spectral analysis.



Scheme 1. Reagents and conditions: (i) anhydrous potassium carbonate, acetone, 0 °C, rt, 4 h, 65-82%; (ii) appropriate sulfonyl chloride derivative, Et₃N, anhydrous THF, 0 °C, rt, 2 h, 43-91%.

2.2. Structure-activity relationship

The target compounds **1a-zk** were tested for inhibitory effects against NPP1, 2, and 3 isozymes. These compounds differed in substitution at linkers R^1 and R^2 (**Table 1**). Six series of compounds were synthesized with R^1 equals cyclopentyl, cyclohexyl, cycloheptyl, cyclooctyl, *p*-chlorophenyl, or 2-naphthyl moiety, diverging with reference to terminal R^2 that was subjected to variable aliphatic or aromatic substituents keeping R^1 with constant structural moiety. These derivatives were analyzed against three forms of NPPs by using colorimetric method with an artificial substrate *p*-Nph-5'-TMP.^{48,49}

Table 1. Structures of the target sulfonate derivatives **1a~zk** and their inhibitory activities (IC_{50} , μM) or inhibition% at 100 μM concentration against NPP1, NPP2, and NPP3.

Codes	R^1	R^2	$IC_{50} \pm SEM$ (μM)/% inhibition		
			NPP1	NPP2	NPP3
1a	Cyclopentyl	Ph	46.67 \pm 0.026	38%	1.724 \pm 0.002
1b	Cyclopentyl	4-Me(C ₆ H ₄)	8.137 \pm 0.003	13.57 \pm 0.001	0.856 \pm 0.003
1c	Cyclopentyl	4- <i>tert</i> -butyl(C ₆ H ₄)	1.648 \pm 0.032	42%	2.675 \pm 0.001
1d	Cyclopentyl	4-F(C ₆ H ₄)	5.76 \pm 0.004	1.473 \pm 0.003	1.014 \pm 0.008
1e	Cyclopentyl	4-CF ₃ (C ₆ H ₄)	1.134 \pm 0.002	0.659 \pm 0.007	3.963 \pm 0.023
1f	Cyclohexyl	Me	1.918 \pm 0.004	33%	1.354 \pm 0.005
1g	Cyclohexyl	Et	1.629 \pm 0.006	1.824 \pm 0.008	0.369 \pm 0.004
1h	Cyclohexyl	<i>n</i> -Pr	3.461 \pm 0.030	26.21 \pm 0.002	2.409 \pm 0.011
1i	Cyclohexyl	Ph	11.85 \pm 0.011	23.76 \pm 0.68	1.079 \pm 0.002
1j	Cyclohexyl	4-Me(C ₆ H ₄)	43%	27%	39%
1k	Cyclohexyl	4- <i>tert</i> -butyl(C ₆ H ₄)	2.55 \pm 0.079	39%	0.807 \pm 0.001
1l	Cyclohexyl	4-F(C ₆ H ₄)	0.564 \pm 0.008	37%	0.254 \pm 0.004
1m	Cyclohexyl	4-CF ₃ (C ₆ H ₄)	0.387 \pm 0.007	1.6 \pm 0.46	1.79 \pm 0.005
1n	Cycloheptyl	Ph	13.84 \pm 0.005	28%	6.602 \pm 0.001
1o	Cycloheptyl	4-Me(C ₆ H ₄)	0.422 \pm 0.008	24%	0.255 \pm 0.007
1p	Cycloheptyl	4- <i>tert</i> -butyl(C ₆ H ₄)	1.493 \pm 0.003	3.908 \pm 0.003	47.01 \pm 0.15
1q	Cycloheptyl	2,4,6-triisopropylphenyl	29%	23%	37%
1r	Cycloheptyl	4-F(C ₆ H ₄)	39.3%	4.944 \pm 0.004	2.267 \pm 0.001
1s	Cycloheptyl	4-CF ₃ (C ₆ H ₄)	0.431 \pm 0.007	34%	2.578 \pm 0.006
1t	Cyclooctyl	Ph	45%	65.36 \pm 1.26	47%
1u	Cyclooctyl	4-Me(C ₆ H ₄)	43%	80.25 \pm 2.12	35%
1v	Cyclooctyl	4- <i>tert</i> -butyl(C ₆ H ₄)	40%	49%	46%
1w	Cyclooctyl	2,4,6-triisopropylphenyl	30%	46%	30%

1x	Cyclooctyl	4-CF ₃ (C ₆ H ₄)	29%	0.679 ± 0.007	0.214 ± 0.012
1y	4-Cl(C ₆ H ₄)	Ph	9.614 ± 0.003	> 100	2.772 ± 0.005
1z	4-Cl(C ₆ H ₄)	4-Me(C ₆ H ₄)	1.437 ± 0.006	7.693 ± 0.635	1.624 ± 0.017
1za	4-Cl(C ₆ H ₄)	4- <i>tert</i> -butyl(C ₆ H ₄)	1.799 ± 0.001	31%	1.525 ± 0.006
1zb	4-Cl(C ₆ H ₄)	2,4,6-triisopropylphenyl	0.975 ± 0.001	24%	1.203 ± 0.004
1zc	4-Cl(C ₆ H ₄)	4-F(C ₆ H ₄)	2.897 ± 0.007	19.91 ± 1.7	46%
1zd	4-Cl(C ₆ H ₄)	4-CF ₃ (C ₆ H ₄)	21.57 ± 0.001	1.07 ± 0.28	3.424 ± 0.004
1ze	2-naphthyl	Ph	9.296 ± 0.016	27.97 ± 0.935	20.51 ± 0.002
1zf	2-naphthyl	4-Me(C ₆ H ₄)	24%	7.995 ± 0.009	23%
1zg	2-naphthyl	4- <i>tert</i> -butyl(C ₆ H ₄)	2.195 ± 0.004	38%	49%
1zh	2-naphthyl	2,4,6-triisopropylphenyl	3.429 ± 0.002	42%	2.892 ± 0.008
1zi	2-naphthyl	4-F(C ₆ H ₄)	1.487 ± 0.002	33%	13.52 ± 0.025
1zj	2-naphthyl	4-CF ₃ (C ₆ H ₄)	1.118 ± 0.007	22%	5.426 ± 0.113
1zk	2-naphthyl	8-quinolinyl	37%	2.461 ± 0.004	42%
Suramin ⁴⁸	-	-	8.670 ± 1.030	-	1.270 ± 0.080
LPA ⁴⁹	-	-	-	0.06 ± 0.01	-

The cyclopentyl derivatives **1a-e**

Introduction of cyclopentyl at R¹ and substitution of sulfonate with phenyl ring at position R² of compound **1a**, resulted in promising inhibitory effect on NPP3. Optimal substitution of phenyl at *para* position with electron-donating group, methyl for compound **1b**, enhanced the selectivity for both NPP3 and NPP1, in contrast to compound **1a**, with an IC₅₀ values of 0.856 ± 0.003 and 8.137 ± 0.003 μM, respectively, resulting in the most potent derivative against NPP3 among the cyclopentyl analogues. Compound **1b** also showed inhibition against NPP2, however not selective and less potent, with inhibitory potency of 13.57 ± 0.001 μM. It was suggested that replacement of methyl with bulky and kinetic-stabilizing group, *tert*-butyl, will enhance the activity of the compound **1c**, surprisingly, there was weaker potency against NPP3, with almost 5 times greater active against NPP1, demonstrating that a compound with bulky substituent has more affinity for NPP1 in contrast to NPP3. Replacement of *tert*-butyl with electron-

withdrawing moiety, fluorine atom, for compound **1d**, retrieved the potency towards NPP2 with an $IC_{50} \pm SEM = 1.473 \pm 0.003 \mu M$, however, declined the affinity for NPP1 by 3 folds with little effect on NPP3. Substitution of fluorine element with less electronegative group trifluoromethyl ($-CF_3$) in compound **1e** exhibited 5 folds and 2.3 folds enhanced inhibition towards NPP1 and NPP2, respectively, in contrast to NPP3 showing 3.9 times decreased potency. This compound was the most potent against NPP2 with auspicious $IC_{50} \pm SEM$ values of $0.659 \pm 0.007 \mu M$. In case of compounds **1d** and **1e**, it can be assumed that substitution with electronegative atom increases the activity against NPP2.

The cyclohexyl derivatives 1f-m

Inhibitory potential of the sulfonate derivatives was further evaluated by modification of terminal R^1 with cyclohexyl cyclic ring instead of cyclopentyl. Insertion of methyl group at position R^2 afforded compound **1f**, found favorable inhibitory potency with respect to NPP1 and NPP3 with an $IC_{50} \pm SEM$ values of 1.918 ± 0.004 and $1.354 \pm 0.005 \mu M$, respectively. However, it showed only 33% inhibition against NPP2. Elongation of aliphatic side chain to ethyl moiety developed compound **1g**, resulted in greater inhibitory potential in respect to NPP3 with an $IC_{50} \pm SEM$ values of $0.369 \pm 0.004 \mu M$. The compound **1g** recovered the potency against NPP2 exhibiting an $IC_{50} \pm SEM$ equals $1.824 \pm 0.008 \mu M$, however it retained the potency towards NPP1. Further elongation of the aliphatic side chain length to *n*-propyl (compound **1h**) exerted declined the activity towards all of three isoenzymes to greater extent. This chain was replaced with aromatic component, phenyl in compound **1i**, which showed less activity to NPP1, NPP2 only $11.85 \pm 0.011 \mu M$ and $23.76 \pm 0.68 \mu M$, respectively but promising effect towards NPP3 representing an IC_{50} values of $1.079 \pm 0.002 \mu M$. Further substitution of phenyl at position 4 with electropositive element, methyl for compound **1j**, declined the activity against all the three isoenzymes with less than 50% inhibition, in contrast to compound **1b** that was active against all of three isozymes. This difference might be due to the increase in carbon in the cyclic ring at R^1 which produced steric hindrance and decreased the affinity of compound towards the enzymes. However, replacement of methyl with 4-(*tert*-butyl) in **1k** stabilized the compound and recovered the inhibitory activity against NPP1 and NPP3 with an $IC_{50} \pm SEM$ of 2.55 ± 0.079 and $0.807 \pm 0.001 \mu M$, respectively. Further replacement of *tert*-butyl with

electronegative atom fluorine, enhanced the inhibitory ability of compound **1l** for NPP1 and NPP3 up to 4.5 folds. Introduction of slightly less electronegative group trifluoromethyl, in place of fluorine, in structure **1m**, resulted in stronger potency against NPP1 and NPP2 but weaker activity against NPP3. It is noteworthy that compounds **1b** and **1f-m** were previously tested against steroid sulfatase enzyme but showed no promising inhibitory effect.⁵⁰

The cycloheptyl derivatives 1n-s

Substitution at place R¹, was moved to greater carbon atoms, cycloheptyl and R² with aromatic ring phenyl, gave rise to compound **1n** that was evaluated against NPP1, NPP2 and NPP3, resulted in weaker potency against all three isozymes than compound **1i** with similar side moiety, phenyl at R². It might be assumed that increase in the carbon atoms in cyclic ring at R¹ did not contribute towards the affinity to greater extent. The substitution of phenyl at *p*-position with methyl in compound **1o** gave the outstanding results for NPP1 with promising IC₅₀ value of 0.422 ± 0.008 μM. It could be proposed that *para* substitution of phenyl ring with some electropositive radical such as methyl, as in compounds **1b**, **1j**, and **1o**, may produce considerable potential for NPPs 1, 2, 3 by balancing the inductive electron-withdrawing effect of the phenyl ring because of sp² hybridization of carbon atoms and stabilizing the compounds. Replacement of methyl substituent with a bulky group, *tert*-butyl in compound **1p**, revealed increased activity against NPP2 to the IC₅₀ values of 3.908 ± 0.003 μM, adding to the concept that more bulky substitution was also effective against NPP2 and not only against NPP1 and NPP3 in accordance with **1c** and **1k**. It was evaluated by replacing it with more spacious group 2, 4, 6-triisopropyl for a compound **1q**. Unexpectedly, activity against all the isoenzymes was less than 50%. It may be suggested that the increase in proportion of electron-donating groups and/or the bulkiness was detrimental for the activity. Substitution of the phenyl ring with electron-withdrawing element in compound **1r**, supported the suggestion to boost the affinity same like **1d** and **1l**, with considerably potency against NPP2 and NPP3 yielding IC₅₀ ± SEM value 4.944 ± 0.004 and 2.267 ± 0.001 μM, respectively, with a much lower activity against NPP1 that was only 39.3%. Further changes in substitution at this position with less effective electron-withdrawing group (–CF₃) at *para* position of phenyl ring, yielded the compound **1s**, which exhibited remarkable activity against NPP1 with IC₅₀ value of 0.431 ± 0.007 μM. However, no

change in activity against NPP3 in contrast to **1r** and revealed just 34% inhibition in case of NPP2.

The cyclooctyl derivatives 1t-x

The compounds **1t-x** of this series were synthesized with increasing carbon atoms in cyclic ring at position R¹ to 8 (cyclooctyl) and substituting the same groups at position R² as for earlier in particular phenyl, *p*-methylphenyl, *p*-(*tert*-butyl)phenyl, 2,4,6-triisopropylphenyl and *p*-(trifluoromethyl)phenyl. These compounds did not manifest describable potential for either of three isoenzymes except compound **1x**. Compound **1x** possessing *p*-(trifluoromethyl)phenyl was found the most potent and active against NPP2 and NPP3 among these synthesized sulfonate derivatives. For NPP2, it exhibited IC₅₀ ± SEM value of 0.679 ± 0.007 μM. It can be suggested that presence of 8-carbon saturated ring contributed to the hydrophobicity of the compound **1x**, made it more selective for NPP2. The compound, **1x** was the most favorable for NPP3 showing an IC₅₀ ± SEM value of 0.214 ± 0.012 μM that was ~6 fold more effective as compared to reference inhibitor, suramin. It was assumed that substitution of electronegative electron-withdrawing group on *para* position of phenyl ring, make the unsaturated ring more accepted for π-π interactions inside the active pocket of isozymes NPP3.

The p-chlorophenyl derivatives 1y-zd

Compounds **1y-zd** were synthesized by substituting the *p*-chlorophenyl at position R¹ and different groups at place R² in particular phenyl, *p*-methylphenyl, *p*-(*tert*-butyl)phenyl, 2,4,6-triisopropylphenyl, *p*-fluorophenyl and *p*-(trifluoromethyl)phenyl, respectively. All these compounds demonstrated encouraging results suggesting that placement of electron-withdrawing substituent at *para* position of cyclic ring has greater influence towards the activity. The compounds **1z**, **1za**, **1zb** revealed favorable potential for NPP1 with an IC₅₀ ± SEM = 1.437 ± 0.006, 1.799 ± 0.001, and 0.975 ± 0.001 μM, respectively and at the same time these compounds were active against NPP3 with an IC₅₀ ± SEM values of 1.624 ± 0.017, 1.525 ± 0.006, and 1.203 ± 0.004 μM, respectively. Among these three only compound **1z** exhibited affinity for NPP2

with an $IC_{50} \pm SEM$ values of $7.693 \pm 0.635 \mu M$. Involvement of electronegative substitutes on both sides R^1 , R^2 as for compounds **1zc** and **1zd** resulted in selective potency. Differentiation of results among 4-chlorobenzene substituted sulfonate derivative **1zc** and cycloheptyl substituted compound **1r** with similar attachment at sulfonate group 4-fluorophenyl, delineated contrary effects against all the three isozymes. Compound **1zc** depicted considerable affinity for NPP1 facing the $IC_{50} \pm SEM = 2.897 \pm 0.007 \mu M$, while compound **1r** showed only 39% inhibition. On the other hand, compound **1r** represented potential against NPP2 and NPP3 with an $IC_{50} \pm SEM = 4.944 \pm 0.004$ and $2.267 \pm 0.001 \mu M$, respectively, while compound **1zc** was less active towards NPP2 and NPP3. This might be due to presence of 4-chloro attachment on phenyl ring, induced the negative inductive property in compound **1zc**, making it more stable and favorable for NPP1 as compared to NPP2. The compound **1zd** was found among the most potent structures against NPP2 with $IC_{50} \pm SEM = 1.07 \pm 0.28 \mu M$.

The 2-naphthyl derivatives 1ze-zk

A new combination of sulfonate derivatives were synthesized by adding bicyclic weak electron donating group, 2-naphthyl, at position R^1 and different types of groups in place of R^2 . 2-Naphthyl was considered as privileged unit for NPPs inhibition. Placement of phenyl linker at point R^2 in compound **1ze**, manifested weak potency. Further substitution of phenyl with introduction of electropositive methyl group in compound **1zf**, re-attained the inhibitory potential for NPP2 with an $IC_{50} \pm SEM$ values of $7.995 \pm 0.001 \mu M$, however, there was further decrease in potency against NPP1 and NPP3. Surrogating the R^2 with divergent groups as an illustration *p*-(*tert*-butyl)phenyl, 2,4,6-triisopropylphenyl, *p*-fluorophenyl, *p*-(trifluoromethyl)phenyl produced the compounds **1zg-1zj**, respectively. These compounds were less than 50% inhibitor against NPP2, although endowed favorable results against NPP1 and NPP3. The compounds **1zi** and **1zj** substituted with electron withdrawing groups, were more potent against NPP1 in contrast to NPP3 with an $IC_{50} \pm SEM = 1.487 \pm 0.002$ and $1.118 \pm 0.007 \mu M$, respectively. The most feasible inhibition against NPP2 of these naphthyl derivatives was attained when R^2 was positioned with 8-quinolinyl group in compound **1zk**. Its inhibitory potency was found among the most selective and potent compounds for NPP2 with an $IC_{50} \pm SEM$ value of $2.461 \pm 0.004 \mu M$.

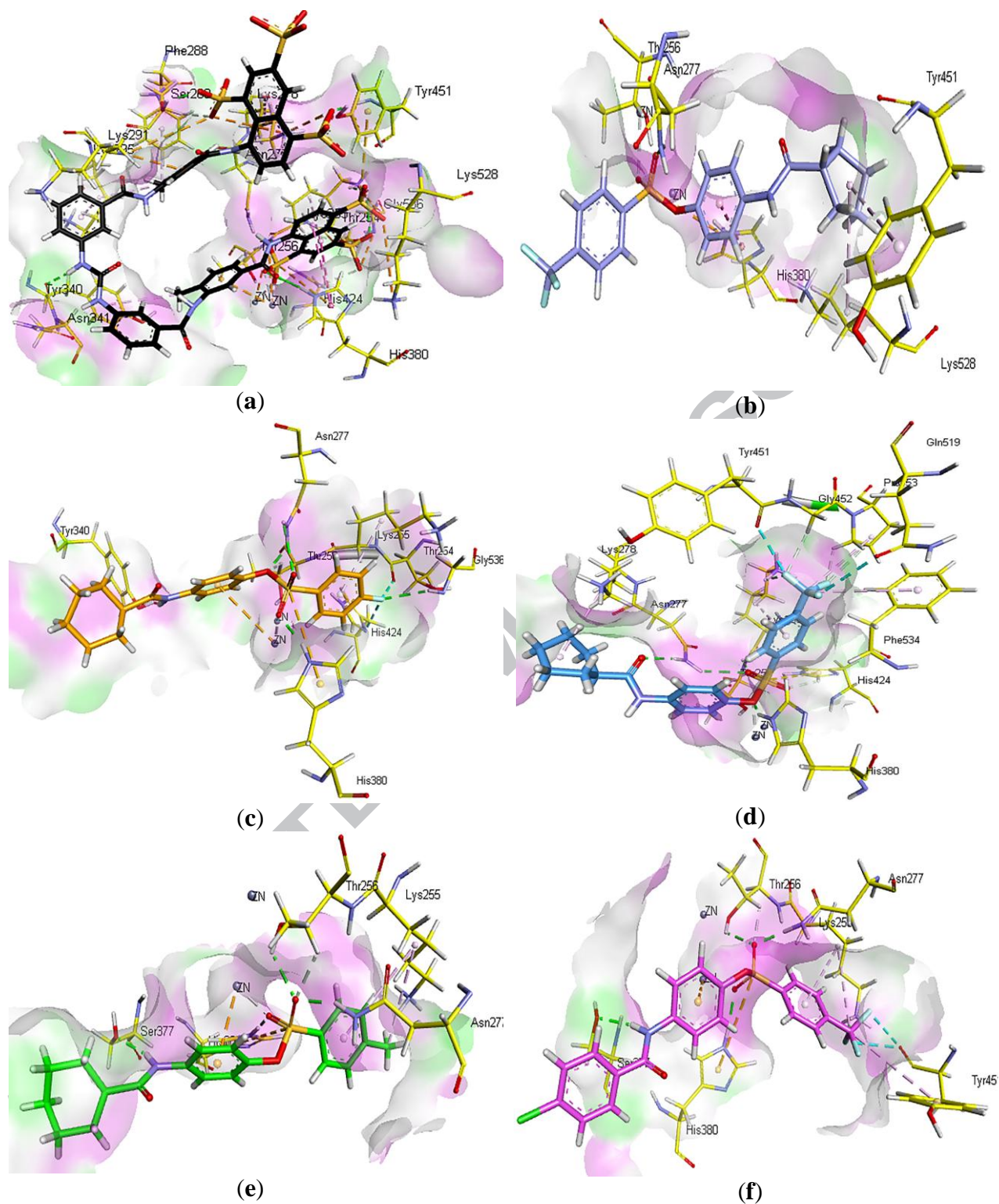
2.3. *Molecular docking studies*

The experimental results suggested that few of the compounds were selective inhibitors of NPP1, 2 and 3, however, some of the compounds exhibited dual inhibition for NPP1 and NPP2, or NPP1 and NPP3 and some also were found active against NPP2 and NPP3. Therefore, docking studies were carried out for all these potent inhibitors having selectivity towards respective isozyme or showing dual inhibition. As the crystal structure of the human nucleotide pyrophosphatases (NPP1) is not available at protein data bank, the docking studies were performed in the homology model generated by our group using mouse ENPP1 with PDB ID: 4B56 as template.⁵¹⁻⁵³ However, the human crystal structures of NPP2 and NPP3 were downloaded from protein data bank with the PDB IDs 4ZG6⁵⁴ and 6C01.⁵⁵ In order to validate the docking studies, the reference compound suramin was docked inside the homology model of human NPP1 and crystal structure of human NPP3. However, the co-crystallized ligand **4NY** (Figure 3a) was extracted and docked inside the crystal structure of NPP2 (4ZG6). The validation was carried out before performing the docking studies of selected compounds for each isozyme. After docking, the root mean square deviation of 0.71 Å was found for co-crystallized ligand, 4NY of NPP2. While for NPP1 (homology model) and NPP3 (6C01), the positive compound suramin was docked and the binding interactions were compared with selected compounds. After the validation process, the docking studies were carried out.

2.3.1. *Docking studies of hNPP1 inhibitors*

The docking studies of NPP1 were carried out for compounds **1e**, **1l**, **1m**, **1o**, **1zd** and **1zj** in addition to suramin. The 3D binding poses for all the selected compounds are shown in Figure 2. The interaction diagram of suramin showed that the amino acids involved in the hydrogen bonding were Lys295, Lys255, Trp307, Lys338, Tyr340, Lys291, Asn277, Lys528 and Thr256 with the oxygen atoms of suramin. However, the π - π interactions were noticed between the phenyl group of suramin and His424, Pro323, Trp322, Ser325, and Asp218. In addition to these interactions, the metal interactions were noticed between two zinc atoms of the active site within the NPP1 and the oxygen atom of suramin. When the detailed investigation of the compound **1e**

was carried out, the most noticeable interactions were hydrogen bonding and metal interactions within the active pocket of NPP1. The trifluoromethyl group was inclined more towards outer region of active pocket, however, the carboxamido group was found to involve in metal interactions with zinc atoms in addition to π - π interaction with His380. The cyclopentyl moiety was found to make π - π interactions with Tyr451 and Lys528. The carboxamido group was located in the middle of the active site of NPP1. When the interactions of the compound **1l** (Figure 2c) were examined, it was found that phenyl ring was interacting with one zinc atom, whereas, oxygen atom of carboxamide part has showed metal interactions with second zinc atom. The fluorine atom at phenyl ring was showing hydrogen bonds with Lys255, Thr254, Gly536 and in addition to hydrogen bond, π - π interactions were observed between His424 and fluorophenyl ring. Compound **1m** (Figure 2d) showed metal interactions with both the zinc atoms present in the active site of NPP1. However, hydrogen bonding were noticed between Gly452, Tyr451, Phe534 and 4-(trifluoromethyl)benzenesulfonate moiety. Moreover, the Asn277 was also involved in hydrogen bonding with carboxamide part of the compound **1m**. The π - π interactions were observed between the cyclohexyl group and Lys278. Upon investigating the docking pose of compound **1o** (Figure 2e), the important interactions found were the metal interactions of zinc ion with central phenyl moiety in addition to oxygen of carboxamide part. Methylbenzenesulfonate moiety showed hydrogen bonding with Lys255 along with π - π interactions with Asn277. When the other compound **1zd** (Figure 2f) was taken into account, the noticeable interactions were shown by important amino acids of the active site and 4-(trifluoromethyl)benzenesulfonate moiety of the compound. The hydrogen bonding were important with residues Tyr451 and Lys255. Moreover, π - π interactions were found Lys255. His380 and Tyr451 were involved in π -phenyl interactions. In case of compound **1zj** (Figure 2g), the 2-naphthamido part was oriented towards the Glu373 and Ser377, whereas, the 4-(trifluoromethyl)benzenesulfonate moiety was found deeper inside the active pocket near the amino acids, Tyr451, Lys255, Thr256 and Asn277. Moreover, the phenyl group in the middle of the compound exhibited arene-cation interaction with zinc present inside the active site of NPP1.



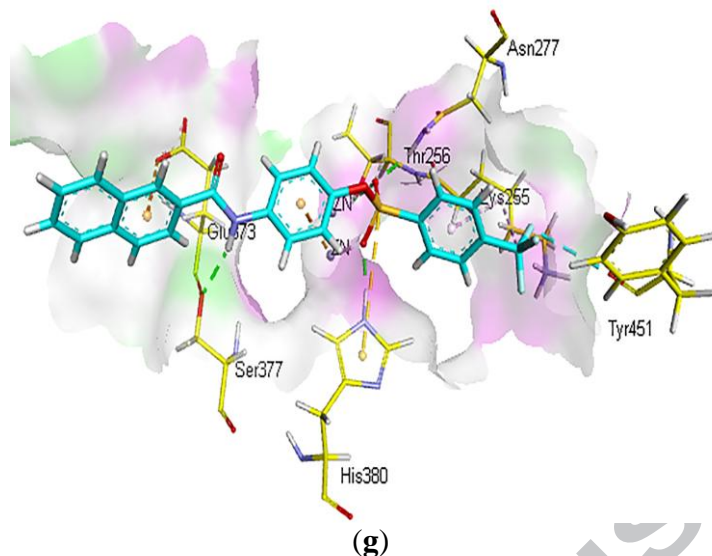
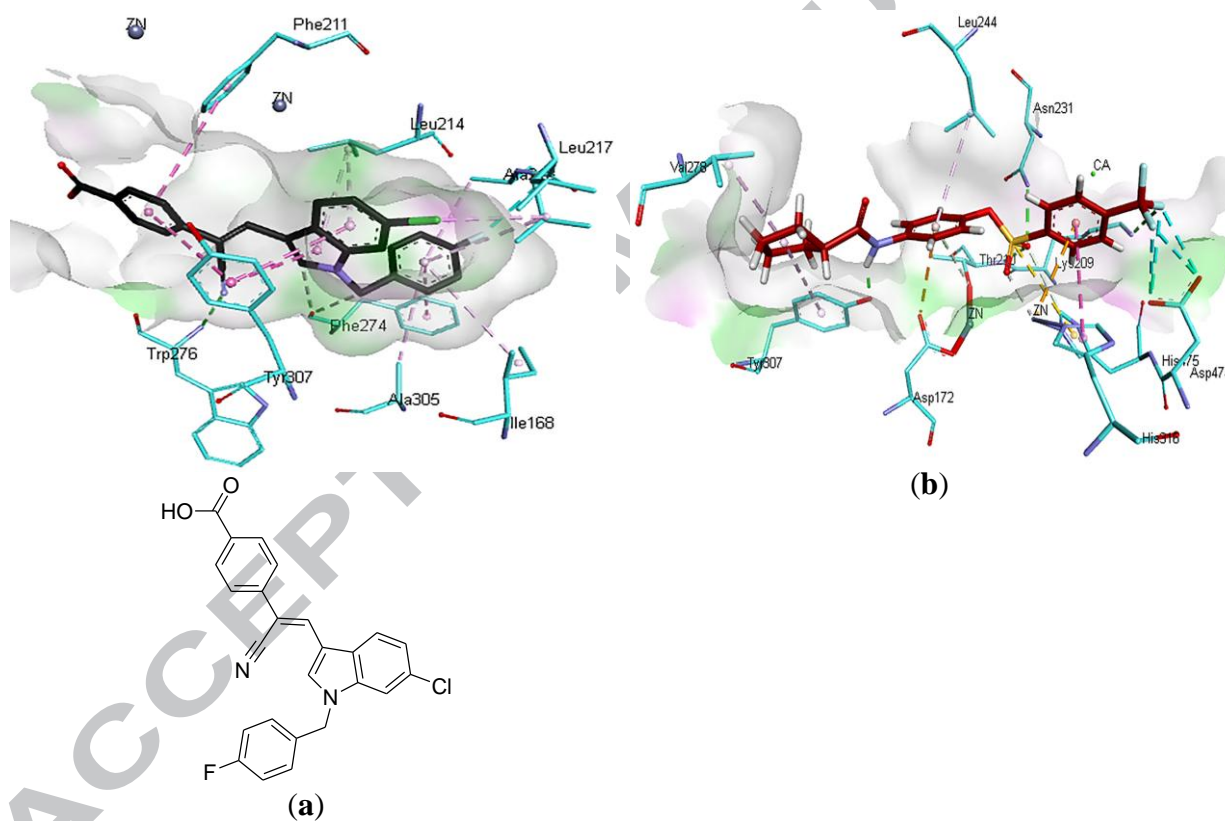


Figure 2. 3D interaction poses (with hydrogen bond surface) of the selective inhibitors of human NPP1 (inside the homology model) (a): **Suramin**; (b): **1e**; (c): **1l**; (d): **1m**; (e): **1o**; (f): **1zd** and (g): **1zj**

2.3.2. Docking studies of hNPP2 inhibitors

The docking studies of NPP2 were carried out for **1e**, **1g**, **1x** and **1zk** in addition to co-crystallized ligand 4NY. The 3D binding poses for all the selected compounds are illustrated in Figure 3. The cognate ligand **4NY** (Figure 3a) of the crystal structure of NPP2 (4ZG6) showed that the important amino acid residues involved in the formation of interactions were Leu214, Phe211, Phe274, Tyr307, Leu217 and Ala218.⁵⁴ Among them, Phe274 and Leu217 were showing hydrogen bonding with cognate ligand. However, the amino acid residues involved in the π - π interactions were Trp276, Tyr307, Ala305, Leu217, Leu214, Phe211 and Phe274. When the compound **1e** was examined for the favorable interactions within the active site (Figure 3b), similar types of interactions were observed as found with the cognate ligand inside the active pocket. The 4-(trifluoromethyl)benzenesulfonate moiety was in π - π interactions with the His316, His475, Asp474, and interactions with zinc atoms. The hydrogen bonding was noticed with His475 and 4-(trifluoromethyl)benzenesulfonate. Another hydrogen bond was noticed between the carboxamido moiety of the compound and His316. The compound **1g**, after docking inside the active pocket, showed the interaction pose depicted in Figure 3c. The oxygen atoms of the compound was found in hydrogen bonding with Asn231. Whereas, π - π interactions of compound were noticed by Leu244, His475, His316, Tyr307 and Val278. The ethanesulfonate group of the

compound **1g** was found towards the zinc atoms inside the active pocket. However, the 4-cyclohexanecarboxamido moiety was oriented towards the Tyr307 and Val278. The compound **1x** (Figure 3d) showed hydrogen bonding with Phe211 and Lys249 by its trifluoromethyl moiety, while with the same phenyl group of **1x**, Phe275 and Phe250 were making the π - π interactions. The cyclooctanecarboxamido moiety was only involved in the formation of π - π interactions with Ala271. When the binding mode of compound **1zk** was examined (Figure 3e), the most noticeable interactions were hydrogen bonding with Trp276, in addition to several π - π interactions with Trp255, Phe274, Tyr307 and Phe275. The zinc atoms did not show any interactions in case of compound **1zk**.



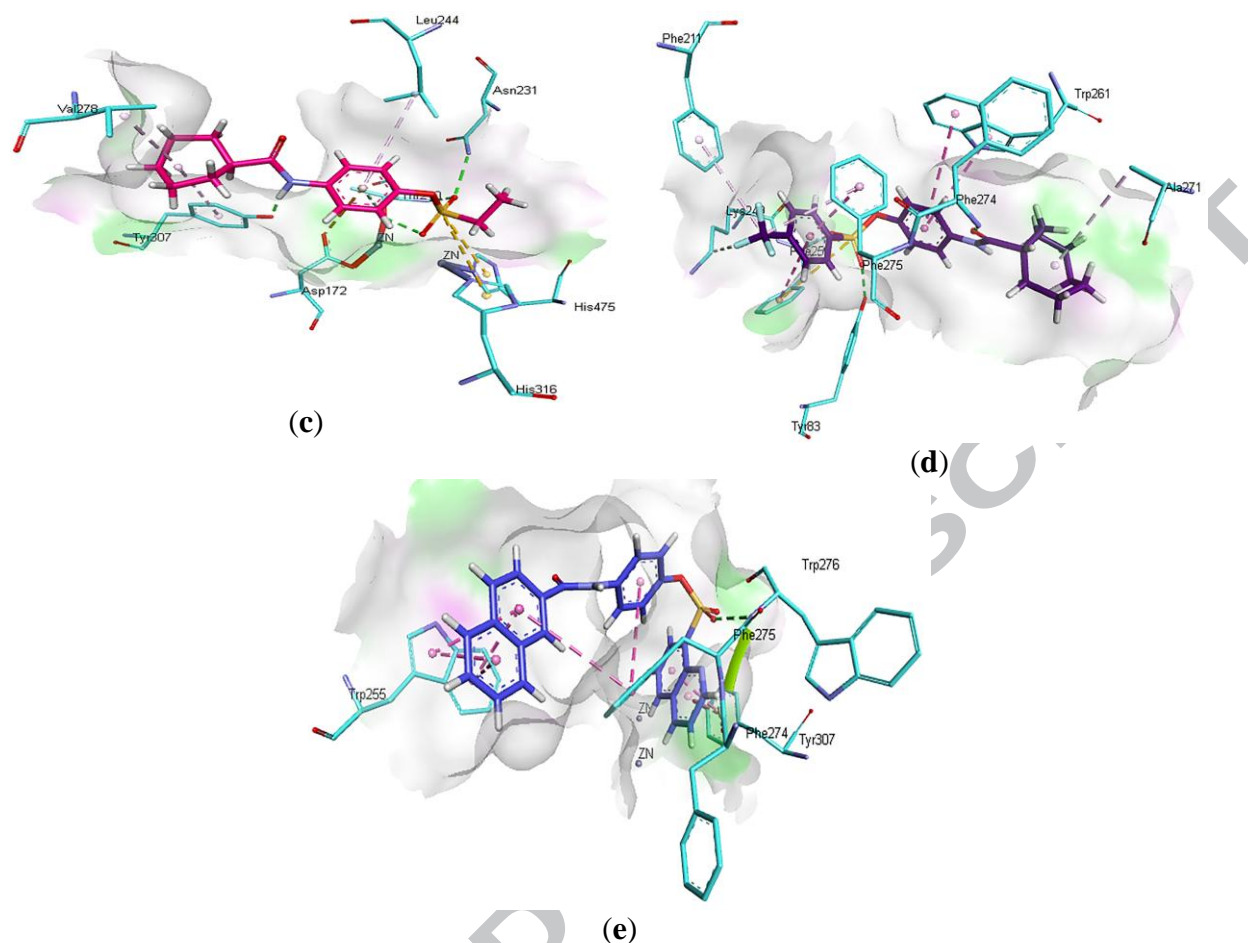


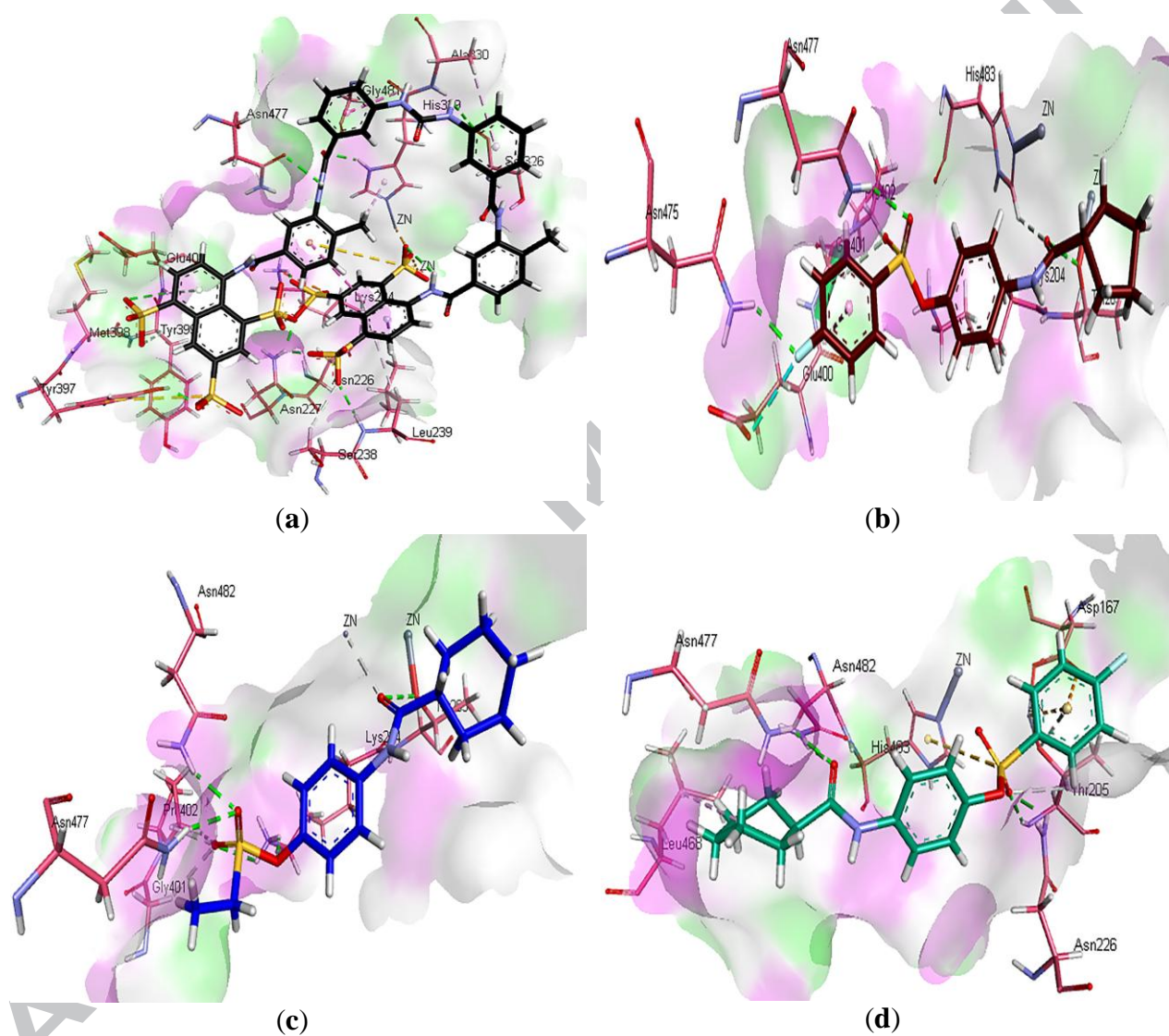
Figure 3. 3D interaction poses (with hydrogen bond surface) of the selective inhibitors of human NPP2 (inside the PDB ID: 4ZG6) (a): **4NY** and its structure; (b): **1e**; (c): **1g**; (d): **1x** and (e): **1zk**

2.3.3. Docking studies of hNPP3 inhibitors

The docking studies of NPP3 were carried out for **1d**, **1g**, **1l**, **1r**, **1x**, **1zd**, and **1zh** in addition to suramin. The 3D binding poses for all the selected compounds are shown in Figure 4. The docking studies of suramin (Figure 4a) inside the active pocket of NPP3 (6C01) revealed that the most important amino acid residues involved in the interactions were His483, His329 and Asp325 coordinated to one of zinc atom, while, Asp372, His373, Thr205 and Asp167 were found in coordination to second zinc atom.⁵⁵ Due to the bulkier structure of suramin, the interactions are noticed in wide active site of the enzyme's pocket. Similarly, many interactions are noticed such as hydrogen bonding, π - π interactions, metal interactions, and π -alkyl

interactions. Compound **1d** (Figure 4b) showed hydrogen bonding with Asn477, Asn475, Glu400, Lys204, Gly401 and His483. However, the π - π interactions were found between Glu400 and 4-fluorobenzenesulfonate group. When the interactions of compound **1g** (Figure 4c) were taken into account, the 3D diagram suggested that the cyclohexanecarboxamide was found more towards the middle of active pocket towards the zinc atoms and showed metal interactions. Hydrogen bonding were observed by the ethanesulfonate group with Asn482, Asn477, Gly401 and Pro402. The 4-fluorobenzenesulfonate moiety of compound **1l** (Figure 4d), more like the compound **1d**, was found deep inside the active pocket exerting similar interactions with side residues including Asp167, Thr205 and Asn226 giving rise to important π - π interactions and hydrogen bonding. Moreover, the cyclohexanecarboxamido group was found profoundly located near amino acids Leu468, Asn477 and Asn482. The phenyl ring located in the center of the compound and the enzyme pocket and was located parallel to the amino acid residues His483 and Asn482. Compound **1r** (Figure 4e) possessing cyclohexanecarboxamide ring showed more or less similar pattern of binding inside the active pocket of NPP3 to that of compound **1d**. However, the cyclopentane ring was replaced by cyclohexane ring and therefore, the 4-fluorobenzenesulfonate was found deeper inside the active pocket towards the important amino acids and showing π - π interactions with Gly401. Moreover, hydrogen bonds were noted by fluorine atom with Glu400 and Asn475. However, the oxygen was making metal interaction with one of the zinc atom inside the active pocket. The compound **1x** (Figure 4f) was monitored, the notable interactions were hydrogen bonding of trifluoromethyl group with Asn475, Glu400 and Pro402. However, the Gly401 was involved in π - π interactions with the compound. Oxygen atom showed metal interactions with both the zinc atoms in addition to Thr205. Moreover, compound **1zd** (Figure 4g) having 4-(trifluoromethyl)benzenesulfonate group was investigated after docking inside the active pocket of NPP3 and the noticeable interactions were hydrogen bonding with Asn477, Asn475, Glu400, Asn482 and Pro402. The 4-chlorobenzamido group of the compound showed π - π interactions with Tyr320, Tyr289, Asp167 and hydrogen bond with Lys204 and Leu239. When compound **1zh** (Figure 4h) from the 2-naphthyl series was taken into account, the 2,4,6-triisopropylbenzenesulfonate moiety was inclined within the pocket of enzyme and showing several π - π interactions with Asn477 and Asn482. However, the important part of the compound, 2-naphthamido moiety exhibited π - π interactions with Thr205 and therefore both sides of this compound exhibited several interactions with the amino acids of active pocket.

The overall docking studies were in accordance with the results of *in vitro* studies and the binding affinities and interactions were following the experimental results. Therefore, both the results are well matched, and justification by docking studies have been provided for the *in vitro* experiments.



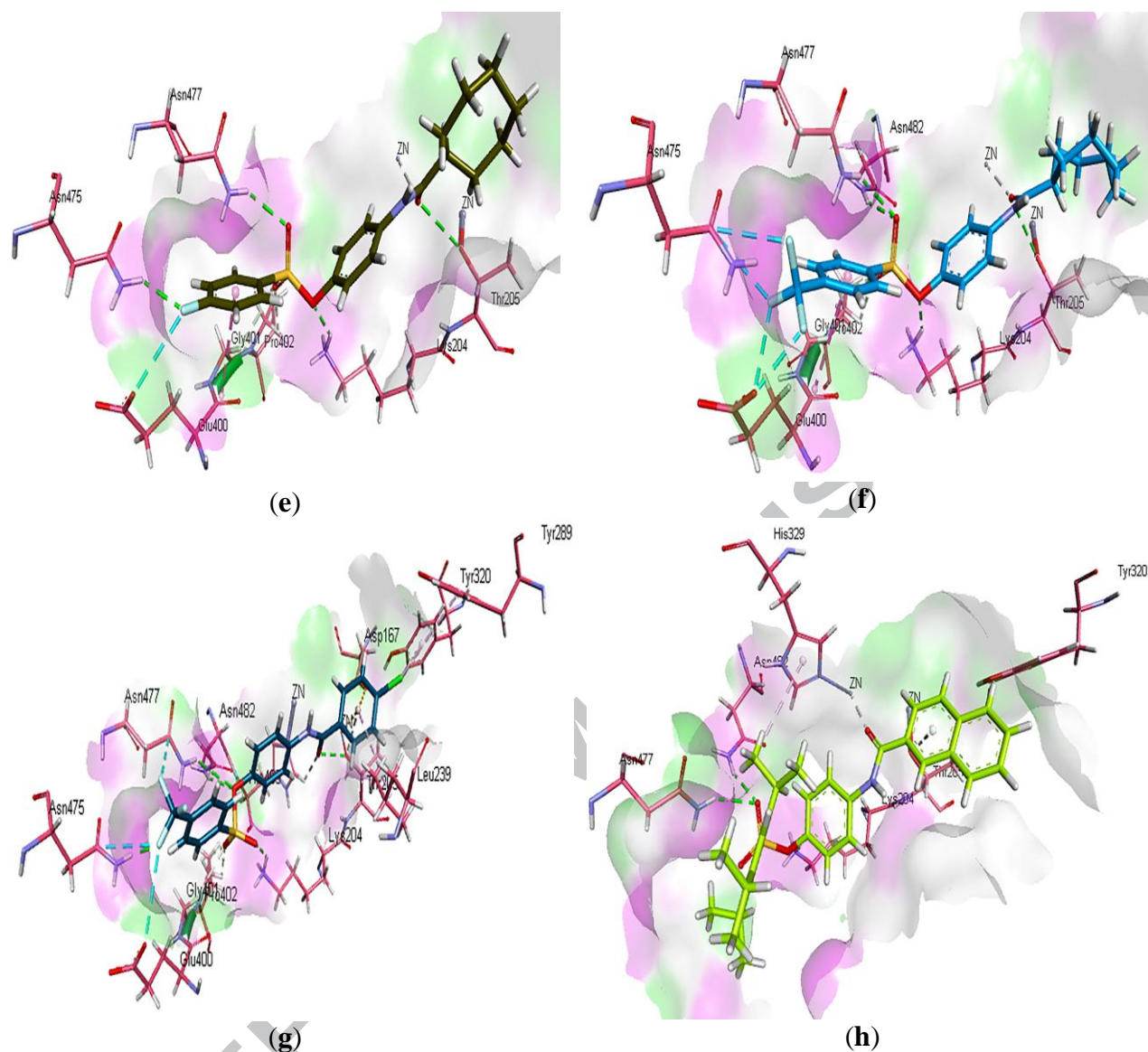


Figure 4. 3D interaction poses (with hydrogen bond surface) of the selective inhibitors of human NPP3 (inside the PDB ID: 6C01) (a): **Suramin**; (b): **1d**; (c): **1g**; (d): **1l**; (e): **1r**; (f): **1x**; (g): **1zd** and (h): **1zh**

HYDE assessment of selective and potent compounds against *h*-NPP1, *h*-NPP2 and *h*-NPP3

The HYDE affinity assessment was done by using LeadIT for the first 30 top ranking docked conformations within the active sites of the homology models of human NPP1, crystal structure of NPP2 and NPP3 and it helped in the selection of correct binding mode as well as the selectivity towards the most potent compound. The FlexX docking score for the selective

derivatives and their binding free energy ΔG were given in Table 2. The FlexX docking score presented the lower energy scores. Moreover, the binding free energies ΔG given in Table 2 showed that the potent inhibitors exhibited higher affinity towards their respective target.

Table 2. Docking and Hyde scores and their corresponding ranks by Hyde affinity assessment (*h*-NPP1, *h*-NPP2 and *h*-NPP3)

Code	FlexX score of the top ranking pose	Binding free energy ΔG (kJ mol ⁻¹)
<i>h</i>-NPP1		
1e	-18.28	-23
1l	-20.79	-21
1m	-20.09	-30
1o	-19.15	-30
1zd	-19.37	-26
1zj	-22.67	-10
<i>h</i>-NPP2		
1e	-20.65	-36
1g	-20.17	-35
1x	-20.48	-33
1zk	-34.97	-38
<i>h</i>-NPP3		
1d	-18.25	-12
1g	-16.88	-10
1l	-19.23	-3
1r	-20.04	-18
1x	-17.27	-17
1zd	-16.46	-39
1zh	-24.13	-19

3. Conclusion

The target sulfonate derivatives were screened for their inhibitory activity against NPP1~3. The results suggested some selective and potent inhibitors of NPP1, 2, and 3 isozymes. However, few compounds were found as dual inhibitors and exhibited significant inhibition against more than one isozyme. The docking investigation resulted in putative binding modes of compounds within each receptor, which further strengthen the *in vitro* results. The most promising compounds as well as other

derivatives that will be designed after lead optimization may further be tested in animal models to get insight of the pharmacological investigation.

4. Experimental

4.1. General

The chemicals and solvents were purchased from Sigma-Aldrich or Alfa Aesar. All the chemicals were used without purification. The target compounds were purified by column chromatography using silica gel (0.040-0.063 mm, 230-400 mesh) and technical grade solvents. ^1H NMR and ^{13}C NMR spectra were recorded on a Bruker Avance 400 or 500 MHz spectrometers using tetramethylsilane as an internal standard. IR spectra (KBr disks) were recorded with a Bruker FT-IR instrument (Bruker Bioscience, Billerica, MA, USA). Mass spectra (MS) were taken in ESI mode on a Waters 3100 Mass Detector (Waters, Milford, MA, USA).

4.2. Synthesis of phenolic intermediates **4a-f**

To a solution of *p*-aminophenol (500 mg, 4.58 mmol) in acetone (60 mL), anhydrous potassium carbonate (760 mg, 5.5 mmol), was added. The reaction mixture was stirred at room temperature for 15 minutes, then cooled to 0 °C. A solution of the appropriate acid chloride (4.165 mmol) in acetone (30 mL) was added dropwise to the reaction mixture at 0 °C with continuous stirring. After complete addition, the reaction mixture was stirred at room temperature for 4 h. The reaction mixture was filtered and the filtered solid was washed with acetone (3 x 10 mL). The combined filtrate and wash were evaporated to dryness. The residue was dissolved in ethyl acetate (50 mL) and extracted with dilute HCl. The organic layer was then washed with saline (2 x 30 mL) and dried with anhydrous Na_2SO_4 . The organic solvent was evaporated under reduced pressure to get the intermediate title compounds. They were used in the next steps as such without further purification.

4.3. General procedure for synthesis of the target sulfonate compounds **1a-zk**

The appropriate phenolic intermediate **4a-f** (0.456 mmol) was dissolved in dry THF (10 mL), and the mixture was cooled to 0 °C. Triethylamine (0.25 mL, 2.47 mmol) was added thereto. A solution of appropriate sulfonyl chloride (0.912 mmol) in dry THF (2 mL) was added dropwise to the reaction mixture at 0 °C. The reaction mixture was stirred at room temperature for 2 h until reaction completion. The mixture was quenched with ethyl acetate (10 mL) and water (10 mL). The organic layer was separated and the aqueous layer was extracted with ethyl acetate (3 x 5 mL). The combined organic layer extract was washed with saline (3 x 10 mL) and dried over anhydrous Na₂SO₄. The organic solvent was evaporated under reduced pressure and the crude residue was purified by column chromatography (silica gel, appropriate ratio of hexane: ethyl acetate) to obtain the pure product. The spectral data of compounds **1b** and **1f-m** have been reported in our previous report⁵⁰ and those for the other target compounds are reported herein in details.

Compound 1a: Yield: 86%; ¹H NMR (400 MHz, CDCl₃) δ 7.67-7.62 (m, 4H), 7.48 (d, 2H, *J* = 8.0 Hz), 7.32 (d, 2H, *J* = 8.0 Hz), 6.91 (d, 2H, *J* = 8.0 Hz), 2.72-2.64 (m, 1H), 2.46 (s, 3H), 1.94-1.75 (m, 6H), 1.62-1.59 (m, 2H); ¹³C NMR (100 MHz, CDCl₃) δ 175.1, 145.6, 145.3, 137.4, 132.2, 129.9, 128.6, 122.9, 120.6, 46.5, 30.6, 26.0; LC-MS: *m/z*: 346.1 [*M*⁺ + 1].

Compound 1c: Yield: 90%; ¹H NMR (400 MHz, CDCl₃) δ 7.67 (d, 2H, *J* = 12.0 Hz), 7.61 (brs, 1H), 7.45 (d, 2H, *J* = 8.0 Hz), 7.30 (d, 2H, *J* = 8.0 Hz), 6.87 (d, 2H, *J* = 8.0 Hz), 2.70-2.62 (m, 1H), 1.91-1.73 (m, 6H), 1.60-1.56 (m, 2H), 1.34 (s, 9H); ¹³C NMR (100 MHz, CDCl₃) δ 175.1, 145.4, 145.1, 137.2, 132.0, 129.7, 128.4, 122.7, 120.4, 46.4, 30.5, 29.6, 26.0, 25.6; LC-MS: *m/z*: 401.82 [*M*⁺ + 1].

Compound 1d: Yield: 82%; ¹H NMR (500 MHz, CDCl₃) δ 7.84-7.81 (m, 2H), 7.47 (d, 2H, *J* = 9.0 Hz), 7.22-7.18 (m, 3H), 6.93-6.90 (m, 2H), 2.67-2.64 (m, 1H), 1.94-1.75 (m, 6H), 1.64-1.42 (m, 2H); ¹³C NMR (125 MHz, CDCl₃) δ 174.8, 167.2, 165.1, 145.3, 137.4, 131.6, 123.0, 120.6, 116.7 (d, *J* = 22.6 Hz), 47.0, 30.6, 26.1; LC-MS: *m/z*: 363.66 [*M*⁺ + 1].

Compound 1e: Yield: 85%; ¹H NMR (400 MHz, CDCl₃) δ 7.84-7.81 (m, 2H), 7.46 (d, 2H, *J* = 9.0 Hz), 7.23-7.17 (m, 3H), 6.94-6.90 (m, 2H), 2.69-2.65 (m, 1H), 1.94-1.76 (m, 6H), 1.64-1.45

(m, 2H); ^{13}C NMR (100 MHz, CDCl_3) δ 174.9, 167.3, 165.2, 145.4, 137.4, 131.8, 123.1, 120.7, 116.8, 47.0, 30.5, 26.1; LC-MS: m/z: 413.73 [$\text{M}^+ + 1$].

Compound 1n: Yield: 78%; ^1H NMR (500 MHz, CDCl_3) δ 7.80 (d, 2H, $J = 2.0\text{Hz}$), 7.70-7.68 (m, 1H), 7.54-7.50 (m, 2H), 7.45 (d, 2H, $J = 9.0\text{Hz}$), 7.38 (brs, 1H), 6.87 (d, 2H, $J = 9.0\text{Hz}$), 2.37-2.33 (m, 1H), 1.95-1.90 (m, 2H), 1.80-1.68 (m, 4H), 1.59-1.51 (m, 4H), 1.49-1.42 (m, 2H); ^{13}C NMR (125 MHz, CDCl_3) δ 175.8, 137.4, 135.3, 134.7, 133.0, 129.4, 123.2, 122.9, 120.6, 48.4, 31.7, 29.8, 28.2; LC-MS: m/z: 374.13 [$\text{M}^+ + 1$].

Compound 1o: Yield: 85%; ^1H NMR (500 MHz, CDCl_3) δ 7.67 (d, 2H, $J = 8.0\text{ Hz}$), 7.44 (d, 2H, $J = 9.0\text{ Hz}$), 7.30-7.28 (m, 3H), 6.88 (d, 2H, $J = 9.0\text{ Hz}$), 2.43 (s, 3H), 2.37-2.33 (m, 1H), 1.95-1.90 (m, 2H), 1.80-1.68 (m, 4H), 1.60-1.50 (m, 4H), 1.49-1.42 (m, 2H); ^{13}C NMR (125 MHz, CDCl_3) δ 175.8, 145.6, 145.4, 137.3, 132.3, 130.0, 129.8, 123.0, 120.6, 48.4, 31.7, 28.3, 26.6; LC-MS: m/z: 388.18 [$\text{M}^+ + 1$].

Compound 1p: Yield: 76%; ^1H NMR (500 MHz, CDCl_3) δ 7.71 (brs, 1H), 7.65 (d, 2H, $J = 8.5\text{ Hz}$), 7.45-7.39 (m, 4H), 6.81 (d, 2H, $J = 9.0\text{ Hz}$), 2.32-2.27 (m, 1H), 1.86-1.80 (m, 2H), 1.69-1.59 (m, 4H), 1.49-1.31 (m, 6H), 1.25 (s, 9H); ^{13}C NMR (125 MHz, CDCl_3) δ 176.1, 158.5, 145.2, 137.4, 132.1, 128.3, 126.2, 122.8, 120.6, 48.1, 35.4, 31.5, 31.0, 28.1, 26.5; LC-MS: m/z: 430.35 [$\text{M}^+ + 1$].

Compound 1q: Yield: 72%; ^1H NMR (500 MHz, CDCl_3) δ 7.61 (s, 1H), 7.40 (d, 2H, $J = 9.0\text{ Hz}$), 6.82 (d, 2H, $J = 8.5\text{ Hz}$), 4.01-3.95 (m, 2H), 2.88-2.82 (m, 1H), 2.31-2.27 (m, 1H), 1.85-1.81 (m, 2H), 1.69-1.64 (m, 4H), 1.44-1.38 (m, 7H), 1.23-1.07 (m, 19H); ^{13}C NMR (125 MHz, CDCl_3) δ 175.9, 154.4, 151.2, 145.1, 173.3, 129.6, 124.0, 122.8, 120.6, 48.1, 34.3, 31.5, 29.8, 28.1, 26.5, 24.6, 23.5; LC-MS: m/z: 430.35 [$\text{M}^+ + 1$].

Compound 1r: Yield: 76%; ^1H NMR (500 MHz, CDCl_3) δ 7.83-7.79 (m, 2H), 7.50 (brs, 1H), 7.46 (d, 2H, $J = 9.0\text{ Hz}$), 7.21-7.16 (m, 2H), 6.88 (d, 2H, $J = 5.0$), 2.38-2.34 (m, 1H), 1.95-1.90 (m, 2H), 1.79-1.68 (m, 4H), 1.59-1.50 (m, 4H), 1.49-1.38 (m, 2H); ^{13}C NMR (125 MHz, CDCl_3) δ 175.9, 145.1, 137.5, 131.5, 131.5, 122.9, 120.7, 116.8, 116.6, 48.3, 31.6, 28.2, 26.6; LC-MS: m/z: 392.31 [$\text{M}^+ + 1$].

Compound 1s: Yield: 83%; ^1H NMR (500 MHz, CDCl_3) δ 7.98 (d, 2H, $J = 8.0$ Hz), 7.82 (d, 2H, $J = 8.0$ Hz), 7.50 (d, 2H, $J = 9.0$ Hz), 7.28 (brs, 1H), 6.94 (d, 2H, $J = 8.5$ Hz), 2.41-2.36 (m, 1H), 1.99-1.94 (m, 2H), 1.84-1.49 (m, 10H); ^{13}C NMR (125 MHz, CDCl_3) δ 175.6, 144.9, 138.8, 137.5, 136.0, 129.1, 126.3, 126.3, 124.0, 121.9; LC-MS: m/z : 442.11 [$\text{M}^+ + 1$].

Compound 1t: Yield: 68%; ^1H NMR (500 MHz, CDCl_3) δ 7.82 (d, 2H, $J = 7.0$ Hz), 7.65 (t, 1H, $J = 7.5$ Hz), 7.51 (t, 2H, $J = 8.0$ Hz), 7.44 (d, 2H, $J = 9.0$ Hz), 7.39 (brs, 1H), 6.88 (d, 2H, $J = 9.0$ Hz), 2.41-2.38 (m, 1H), 1.90-1.87 (m, 2H), 1.86-1.75 (m, 4H), 1.61-1.53 (m, 8H); ^{13}C NMR (125 MHz, CDCl_3) δ 176.1, 145.3, 137.4, 135.3, 134.4, 129.3, 128.6, 123.0, 120.7, 46.8, 29.8, 26.7, 26.3, 22.8; LC-MS: m/z : 388.0 [$\text{M}^+ + 1$].

Compound 1u: Yield: 78%; ^1H NMR (500 MHz, CDCl_3) δ 7.68 (d, 2H, $J = 8.5$ Hz), 7.44 (d, 2H, $J = 9.0$ Hz), 7.29 (d, 2H, $J = 8.0$ Hz), 7.24 (brs, 1H), 6.90 (d, 2H, $J = 7.5$ Hz), 2.44 (s, 3H), 2.41-2.38 (m, 1H), 1.92-1.87 (m, 2H), 1.81-1.78 (m, 4H), 1.64-1.57 (m, 8H); ^{13}C NMR (125 MHz, CDCl_3) δ 175.0, 144.5, 144.4, 136.3, 131.3, 128.9, 127.7, 122.1, 119.6, 45.9, 28.8, 25.8, 25.3, 24.6, 20.9; LC-MS: m/z : 402.0 [$\text{M}^+ + 1$].

Compound 1v: Yield: 64%; ^1H NMR (500 MHz, CDCl_3) δ 7.73 (d, 2H, $J = 9.0$ Hz), 7.52 (d, 2H, $J = 7.0$ Hz), 7.45 (d, 2H, $J = 9.0$ Hz), 7.16 (brs, 1H), 6.93 (d, 2H, $J = 8.5$ Hz), 2.42-2.37 (m, 1H), 1.91-1.88 (m, 2H), 1.82-1.75 (m, 4H), 1.63-1.53 (m, 8H), 1.35 (s, 9H); ^{13}C NMR (125 MHz, CDCl_3) δ 176.0, 158.5, 145.5, 137.2, 132.4, 128.5, 126.3, 123.1, 120.6, 120.5, 46.9, 35.5, 31.1, 29.8, 26.7, 26.3, 25.5; LC-MS: m/z : 444.23 [$\text{M}^+ + 1$].

Compound 1w: Yield: 70%; ^1H NMR (500 MHz, CDCl_3) δ 7.38 (d, 2H, $J = 9.0$ Hz), 7.12 (s, 2H), 7.03 (brs, 1H), 6.86 (d, 2H, $J = 9.0$ Hz), 2.36-2.29 (m, 1H), 1.84-1.81 (m, 2H), 1.74-1.68 (m, 4H), 1.55-1.47 (m, 8H), 1.21-1.18 (m, 9H), 1.12 (d, 12H, $J = 7.0$ Hz); ^{13}C NMR (125 MHz, CDCl_3) δ 175.9, 154.4, 151.4, 145.5, 137.1, 129.8, 124.0, 123.1, 120.6, 47.0, 34.4, 29.9, 29.8, 26.8, 26.3, 25.6, 24.7, 23.7; LC-MS: m/z : 514.2 [$\text{M}^+ + 1$].

Compound 1x: Yield: 74%; ^1H NMR (500 MHz, CDCl_3) δ 7.96 (d, 2H, $J = 8.0$ Hz), 7.80 (d, 2H, $J = 8.5$ Hz), 7.48 (d, 2H, $J = 9.0$ Hz), 7.10 (brs, 1H), 6.93 (d, 2H, $J = 8.5$ Hz), 2.41-2.34 (m, 1H), 1.80-1.78 (m, 6H), 1.71-1.53 (m, 8H); ^{13}C NMR (125 MHz, CDCl_3) δ 175.1, 144.6, 144.3, 133.4, 129.3, 126.5, 122.9, 120.8, 45.9, 29.8, 26.8, 25.5, 22.8, 14.3; LC-MS: m/z : 456.0 [$\text{M}^+ + 1$].

Compound 1y: Yield: 81%; ^1H NMR (500 MHz, DMSO- d_6) δ 10.42 (brs, 1H), 7.95 (d, 2H, $J = 8.5$ Hz), 7.87-7.86 (m, 3H), 7.74 (d, 2H, $J = 9.0$ Hz), 7.68 (t, 2H, $J = 8.0$ Hz), 7.61 (d, 2H, $J = 7.0$ Hz), 7.02 (d, 2H, $J = 7.0$ Hz); ^{13}C NMR (125 MHz, CDCl_3) δ 164.6, 144.6, 138.1, 136.6, 135.0, 134.2, 133.3, 129.8, 129.7, 128.5, 128.3, 122.4, 121.5; LC-MS: m/z : 388.0 [$\text{M}^+ + 1$].

Compound 1z: Yield: 78%; ^1H NMR (500 MHz, DMSO- d_6) δ 10.42 (brs, 1H), 7.96 (d, 2H, $J = 8.5$ Hz), 7.74 (m, 4H), 7.61 (d, 2H, $J = 9.0$ Hz), 7.48 (d, 2H, $J = 8.0$ Hz), 7.01 (d, 2H, $J = 9.0$ Hz), 2.43 (s, 3H); ^{13}C NMR (125 MHz, CDCl_3) δ 164.5, 145.8, 144.6, 138.0, 136.6, 133.3, 131.4, 130.2, 129.6, 128.5, 128.3, 122.4, 121.5, 21.2; LC-MS: m/z : 402.0 [$\text{M}^+ + 1$].

Compound 1za: Yield: 76%; ^1H NMR (500 MHz, DMSO- d_6) δ 10.42 (brs, 1H), 7.98-7.95 (m, 2H), 7.81-7.79 (m, 4H), 7.76 (d, 2H, $J = 5.0$ Hz), 7.61 (d, 2H, $J = 9.0$ Hz), 7.04 (d, 2H, $J = 10.0$ Hz), 1.34 (s, 9H); ^{13}C NMR (125 MHz, DMSO- d_6) δ 164.5, 158.2, 144.6, 138.0, 136.6, 133.3, 131.5, 129.6, 128.5, 128.1, 126.7, 122.3, 121.4, 35.2, 30.7; LC-MS: m/z : 444.1 [$\text{M}^+ + 1$].

Compound 1zb: Yield: 85%; ^1H NMR (500 MHz, DMSO- d_6) δ 10.43 (brs, 1H), 7.96 (d, 2H, $J = 8.5$ Hz), 7.77 (d, 2H, $J = 9.0$ Hz), 7.60 (d, 2H, $J = 8.5$ Hz), 7.36 (s, 2H), 6.99 (d, 2H, $J = 9.0$ Hz), 3.96-3.90 (m, 2H), 3.01-2.96 (m, 1H), 1.23 (d, 6H, $J = 7.0$ Hz), 1.15 (d, 12H, $J = 7.0$ Hz); ^{13}C NMR (125 MHz, DMSO- d_6) δ 164.5, 154.6, 150.7, 144.4, 138.0, 136.6, 133.3, 129.7, 128.8, 128.5, 124.1, 122.4, 121.6, 33.5, 29.4, 24.2, 23.3; LC-MS: m/z : 514.15 [$\text{M}^+ + 1$].

Compound 1zc: Yield: 88%; ^1H NMR (500 MHz, DMSO- d_6) δ 10.44 (brs, 1H), 8.09 (q, 4H, $J = 8.5$ Hz), 7.96 (d, 2H, $J = 9.0$ Hz), 7.77 (d, 2H, $J = 9.0$ Hz), 7.61 (d, 2H, $J = 9.0$ Hz), 7.07 (d, 2H, $J = 9.0$ Hz); ^{13}C NMR (125 MHz, DMSO- d_6) δ 164.6, 144.3, 138.4, 138.2, 136.6, 134.5, 133.3, 129.7, 128.5, 127.1, 124.3, 122.4, 121.6; LC-MS: m/z : 406.0 [$\text{M}^+ + 1$].

Compound 1zd: Yield: 90%; ^1H NMR (500 MHz, DMSO- d_6) δ 10.43 (brs, 1H), 7.97-7.93 (m, 4H), 7.77 (d, 2H, $J = 7.0$ Hz), 7.61 (d, 2H, $J = 5.0$ Hz), 7.53 (t, 2H, $J = 8.5$ Hz), 7.04 (d, 2H, $J = 7.0$ Hz); ^{13}C NMR (125 MHz, DMSO- d_6) δ 166.6, 164.5, 144.4, 138.2, 136.6, 133.3, 131.7, 130.5, 129.6, 128.5, 122.4, 121.5, 117.3, 117.1; LC-MS: m/z : 456.0 [$\text{M}^+ + 1$].

Compound 1ze: Yield: 74%; ^1H NMR (500 MHz, CDCl_3) δ 8.38 (brs, 1H), 8.11 (s, 1H), 7.95-7.88 (m, 4H), 7.78 (dd, 2H, $J = 4.5$ Hz, $J = 6.5$ Hz), 7.65-7.50 (m, 7H), 7.03 (dd, 2H, $J = 2.0$ Hz, $J = 7.0$ Hz); ^{13}C NMR (125 MHz, CDCl_3) δ 165.9, 158.5, 145.9, 137.1, 135.1, 132.7, 132.3,

131.9, 129.1, 129.0, 128.5, 128.2, 128.0, 127.8, 127.2, 126.3, 123.6, 123.2, 121.2; LC-MS: m/z: 404.97 [$M^+ + 1$].

Compound 1zf: Yield: 81%; ^1H NMR (500 MHz, CDCl_3) δ 8.39 (brs, 1H), 8.11 (s, 1H), 7.94-7.87 (m, 4H), 7.78 (dd, 2H, $J = 4.5$ Hz, $J = 6.5$ Hz), 7.67-7.51 (m, 6H), 7.04 (dd, 2H, $J = 2.0$ Hz, $J = 7.0$ Hz), 2.43 (s, 3H); ^{13}C NMR (125 MHz, CDCl_3) δ 165.9, 158.5, 145.9, 137.1, 135.1, 132.7, 132.3, 131.9, 129.1, 129.0, 128.5, 128.2, 128.0, 127.8, 127.2, 126.3, 123.6, 123.2, 121.2, 21.2; LC-MS: m/z: 418.08 [$M^+ + 1$].

Compound 1zg: Yield: 85%; ^1H NMR (500 MHz, CDCl_3) δ 8.35 (brs, 1H), 8.10 (s, 1H), 7.93-7.87 (m, 4H), 7.76 (dd, 2H, $J = 4.5$ Hz, $J = 6.5$ Hz), 7.65-7.51 (m, 6H), 7.01 (dd, 2H, $J = 2.0$ Hz, $J = 7.0$ Hz), 1.35 (s, 9H); ^{13}C NMR (125 MHz, CDCl_3) δ 165.9, 158.5, 145.9, 137.1, 135.1, 132.7, 132.3, 131.9, 129.1, 129.0, 128.5, 128.2, 128.0, 127.8, 127.2, 126.3, 123.6, 123.2, 121.2, 35.5, 31.2; LC-MS: m/z: 460.19 [$M^+ + 1$].

Compound 1zh: Yield: 78%; ^1H NMR (500 MHz, CDCl_3) δ 8.35 (brs, 1H), 8.00 (s, 1H), 7.94 (dd, 2H, $J = 5.5$ Hz, $J = 7.0$ Hz), 7.93-7.88 (m, 2H), 7.65 (d, 2H, $J = 10.5$ Hz), 7.63-7.55 (m, 2H), 7.21 (s, 2H), 7.04-7.01 (m, 2H), 4.12-4.07 (m, 2H), 2.97-2.92 (m, 1H), 1.28 (d, 6H, $J = 7.0$ Hz), 1.21 (d, 12H, $J = 7.0$ Hz); ^{13}C NMR (125 MHz, CDCl_3) δ 165.8, 154.5, 151.4, 145.9, 136.9, 135.1, 132.7, 131.9, 129.8, 129.1, 129.0, 128.2, 128.0, 127.7, 127.2, 124.1, 123.5, 123.3, 121.2, 34.4, 30.0, 24.8, 23.7; LC-MS: m/z: 530.19 [$M^+ + 1$].

Compound 1zi: Yield: 87%; ^1H NMR (500 MHz, $\text{DMSO-}d_6$) δ 10.60 (brs, 1H), 8.56 (s, 1H), 8.12-8.02 (m, 8H), 7.84 (d, 2H, $J = 9.0$ Hz), 7.67-7.63 (m, 2H), 7.13 (d, 2H, $J = 9.0$ Hz); ^{13}C NMR (125 MHz, $\text{DMSO-}d_6$) δ 165.8, 144.3, 138.5, 138.1, 134.3, 134.2, 134.1, 132.0, 131.8, 129.2, 129.0, 128.0, 127.7, 127.5, 127.0, 126.6, 124.3; LC-MS: m/z: 422.03 [$M^+ + 1$].

Compound 1zj: Yield: 91%; ^1H NMR (500 MHz, $\text{DMSO-}d_6$) δ 10.58 (brs, 1H), 8.57 (s, 1H), 8.13-8.00 (m, 8H), 7.86 (d, 2H, $J = 9.0$ Hz), 7.65-7.62 (m, 2H), 7.11 (d, 2H, $J = 9.0$ Hz); ^{13}C NMR (125 MHz, $\text{DMSO-}d_6$) δ 165.7, 144.2, 138.6, 138.2, 134.4, 134.3, 134.2, 132.0, 131.9, 129.4, 129.0, 128.1, 127.9, 127.7, 127.1, 127.0, 126.9, 124.4; LC-MS: m/z: 472.14 [$M^+ + 1$].

Compound 1zk: Yield: 43%; ^1H NMR (500 MHz, $\text{DMSO-}d_6$) δ 8.41 (brs, 1H), 8.14 (s, 1H), 7.98-7.89 (m, 7H), 7.82 (dd, 2H, $J = 4.5$ Hz, $J = 6.5$ Hz), 7.68-7.53 (m, 7H), 7.06 (dd, 2H, $J =$

2.0 Hz, $J = 7.0$ Hz); ^{13}C NMR (125 MHz, DMSO- d_6) δ 166.0, 158.5, 145.9, 137.1, 135.1, 133.6, 134.4, 132.7, 132.4, 131.9, 129.2, 129.0, 128.8, 128.5, 128.2, 128.0, 127.9, 127.3, 126.4, 123.7, 123.3, 121.3; LC-MS: m/z : 455.24 [$\text{M}^+ + 1$].

4.4. Nucleotide pyrophosphatase/ phosphodiesterase inhibition assays

The inhibition potential of all the sulfonate derivatives against NPP1, 2, and 3 was determined by considering already reported colorimetric method^{54,55} with minor modifications. The reaction buffer was comprised of 50 mM Tris-hydrochloric acid, 5 mM magnesium chloride (MgCl_2) and 0.1 mM zinc chloride (ZnCl_2) with final pH 9.5. For initial screening of compounds, enzyme and substrate parameters (concentration, temperature, time) were first optimized. The reaction assay was performed at 100 μL well volume containing assay buffer, 10 μL of 1 mM test compound prepared in 10% DMSO, enzymes NPP1 (35 ng), NPP2 (338 ng), or NPP3 (37 ng) and assay buffer. The reaction mixture was incubated at 37 $^\circ\text{C}$, 10 minutes for NPP1 and 3 and 5 minutes for NPP2. Absorbance was measured at wavelength of 405 nm as pre-read by using microplate reader (BioTek FLx800, Instruments, Inc. USA). After pre-read artificial substrate *p*-nitrophenyl 5'-thymidine monophosphate (*p*NP-TMP), 400 μM for NPP1, 500 μM for NPP2, or 600 μM in case of NPP3, was added followed by second incubation at 37 $^\circ\text{C}$, 15 minutes for NPP1, 3 and 35 minutes for NPP2. Absorbance was measured as after read. All the experiments were performed in triplicates. Compounds exhibiting more than 50% inhibition against either of NPP1, NPP2, and NPP3 were further subjected to serial dilutions for the determination of IC_{50} values, using non-linear curve fitting program PRISM 5.0 (Graph Pad, San Diego, California, USA).

4.5. Molecular docking studies

4.5.1. Selection of protein structure

Due to the unavailability of crystal structure of the human nucleotide pyrophosphatases (NPP1), the docking studies were performed in the homology model generated by our group using mouse ENPP1 with PDB ID: 4B56 as template.^{48,50} However, the human crystal structures of NPP2 and NPP3 were downloaded from protein data bank with the PDB IDs 4ZG6⁵¹ and

6C01.⁵² The crystal structures of human NPP2 and NPP3 were present in the form of homodimer chain, therefore chain A was selected for docking analysis. MOE site finder parameter was applied to find out the binding pocket inside respective enzyme, keeping in mind the importance of catalytic zinc ions and calcium ions inside the active site pocket of enzyme.⁵⁶ The structure of these proteins were protonated by AMBER99 force field, and minimization was done at root mean square deviation gradient of 0.05 kcal/mol.⁵⁷

4.5.2. Preparation of the ligands

The 3D structures of the selected compounds were prepared with the help of builder tool of MOE.⁵⁶ After addition of hydrogen atoms to the compounds, the energy was minimized for the prepared structures of ligands and MMFF94x force field at the root mean square deviation of 0.01 kcal/mol Å was used for minimization.⁵⁷

4.5.3. Docking Analysis

The docking studies of the selected inhibitors and the standard compounds were performed with the help of LeadIT (BioSolveIT GmbH, Germany)⁵⁸ by setting the default parameters. The top 50 resulted poses were selected and visualization was done for each inhibitor individually. The top 30 poses were selected for HYDE assessment to further investigate the favorable binding interactions.⁵⁹ The poses having low binding energy with favorable affinity were selected, and analysis was performed using Discovery Studio Visualizer DS.⁶⁰

Acknowledgements

The authors are grateful to University of Sharjah (Drug Design & Discovery Research Group Operational Fund), United Arab Emirates, Boehringer-Ingelheim pharmaceutical company, United Arab Emirates, and Korea Institute of Science and Technology (KIST, Seoul, Republic of Korea), KIST Project (E26900) for financial support. J.I. is thankful to the Organization for the Prohibition of Chemical Weapons (OPCW), The Hague, The Netherlands and Higher Education Commission of Pakistan for the financial support through Project No. 20-3733/NRPU/R&D/14/520. J.S. was supported by grants from the Canadian Institutes of Health

Research. J.S. is also a recipient of a “Chercheur National” Scholarship award from the “Fonds de recherche du Québec-Santé” (FRQS).

References:

- [1] Zimmermann, H.; Zebisch, M.; Strater, N. *Purinergic Signalling* 2012;8:437.
- [2] Ausekle, E.; Ejaz, S.A.; Khan, S.U.; Ehlers, P.; Villinger, A.; Lecka, J.; Sevigny, J.; Iqbal, J.; Langer, P. *Organic & Biomolecular Chemistry* 2016;14:11402.
- [3] Hunsucker, S.A.; Mitchell, B.S.; Sychala, J. *Pharmacology & Therapeutics* 2005;107:1.
- [4] Johnson, K.; Moffa, A.; Chen, Y.; Pritzker, K.; Goding, J.; Terkeltaub, R. *Journal of Bone and Mineral Research* 1999;14:883.
- [5] Stefan, C.; Jansen, S.; Bollen, M. *Purinergic Signalling* 2006;2:361.
- [6] Ciancaglini, P.; Yadav, M.C.; Simao, A.M.; Narisawa, S.; Pizauro, J.M.; Farquharson, C.; Hoylaerts, M.F.; Millan, J.L. *Journal of Bone and Mineral Research* 2010;25:716.
- [7] Harmey, D.; Hessle, L.; Narisawa, S.; Johnson, K.A.; Terkeltaub, R.; Millan, J.L. *The American Journal of Pathology* 2004;164:1199.
- [8] Nitschke, Y.; Hartmann, S.; Torsello, G.; Horstmann, R.; Seifarth, H.; Weissen-Plenz, G.; Rutsch, F. *Journal of Cellular and Molecular Medicine* 2011;15:220.
- [9] Levy-Litan, V.; Hershkovitz, E.; Avizov, L.; Leventhal, N.; Bercovich, D.; Chalifa-Caspi, V.; Manor, E.; Buriakovsky, S.; Hadad, Y.; Goding, J.; Parvari, R. *The American Journal of Human Genetics* 2010;86:273.
- [10] Ruf, N.; Uhlenberg, B.; Terkeltaub, R.; Nurnberg, P.; Rutsch, F. *Human Mutation* 2005;25:98.
- [11] Terkeltaub, R. *Purinergic Signalling* 2006;2:371.
- [12] Sun, Y.; Mauerhan, D.R.; Honeycutt, P.R.; Kneisl, J.S.; Norton, H.J.; Zinchenko, N.; Hanley, E.N.; Gruber, H.E. *Arthritis Research & Therapy* 2010;12:R56.
- [13] Cote, N.; El Husseini, D.; Pepin, A.; Guauque-Olarte, S.; Ducharme, V. *Journal of Molecular and Cellular Cardiology* 2012;52:1191.
- [14] Umezū-Goto, M.; Kishi, Y.; Taira, A.; Hama, K.; Dohmae, N.; Takio, K.; Yamori, T.; Mills, G.B.; Inoue, K.; Aoki, J.; Arai, H. *Journal of Cell Biology* 2012;158:227.

- [15] Mangodt, E.A.; Van Gasse, A.L.; Bastiaensen, A.; Decuyper, I.I.; Uyttebroek, A.; Faber, M.; Sabato, V.; Bridts, C.H.; Hagendorens, M.M.; De Clerck, L.S.; Ebo, D.G. *Acta Clinica Belgica* 2016;71:19.
- [16] Bollen, M.; Gijssbers, R.; Ceulemans, H.; Stalmans, W.; Stefan, C. *Critical Reviews in Biochemistry and Molecular Biology* 2000;35:393.
- [17] Scott, L.J.; Delautier, D.; Meerson, N.R.; Trugnan, G.; Goding, J.W.; Maurice, M. *Hepatology* 1997;25:995.
- [18] Koike, S.; Keino-Masu, K.; Ohto, T.; Masu, M. *Genes to Cells* 2006;11:133.
- [19] Nishimasu, H.; Okudaira, S.; Hama, K.; Mihara, E.; Dohmae, N.; Inoue, A.; Ishitani, R.; Takagi, J.; Aoki, J.; Nureki, O. *Nature Structural & Molecular Biology* 2011;2:205.
- [20] Fulkerson, Z.; Wu, T.; Sunakura, M.; Vander Kooi, C.; Morris, A.J.; Smyth, S.S. *Journal of Biological Chemistry* 2011;286:34654.
- [21] Moolenaar, W.H.; Perrakis, A. *Nature Reviews Molecular Cell Biology* 2011;12:674.
- [22] Yung, Y.C.; Stoddard, N.C.; Chun, J. *Journal of Lipid Research* 2014;55:1192.
- [23] Mills, G.B.; Moolenaar, W.H. *Nature Reviews Cancer* 2003;3:582.
- [24] Bain, G.; Shannon, K.E.; Huang, F.; Darlington, J.; Goulet, L.; Prodanovich, P.; Ma, G.L.; Santini, A.M.; Stein, A.J.; Lonergan, D.; King, C.D.; Calderon, I.; Lai, A.; Hutchinson, J.H.; Evans, J.F. *Journal of Pharmacology and Experimental Therapeutics* 2017;360:1.
- [25] Inoue, M.; Rashid, M.H.; Fujita, R.; Contos, J.J.A.; Chun, J.; Ueda, H. *Nature Medicine* 2004;10:712.
- [26] Bourgion, S.G.; Zhao, C. *Current Opinion in Investigational Drugs* 2010;11:515.
- [27] Hui, D.Y. *Current Opinion in Lipidology* 2016;27:507.
- [28] [a] Kremer, A.E.; van Dijk, R.; Leckie, P.; Schaap, F.G.; Kuiper, E.M.; Mettang, T.; Reiners, E.S.; Raap, U.; van Buuren, H.R.; van Erpecum, K.J.; Davies, N.A.; Rust, C.; Engert, A.; Jalan, R.; Oude Elferink, R.P.; Beuers, U. *Hepatology* 2012;56:1391; [b] Castelino, F.V.; Bain, G.; Pace, V.A.; Black, K.E.; George, L.; Probst, C.K.; Goulet, L.; Lafyatis, R.; Tager, A.M. *Arthritis & Rheumatology* 2016;68:2964.
- [29] Hausmann, J.; Kamtekar, S.; Christodoulou, E.; Day, J.E.; Wu, T.; Fulkerson, Z.; Albers, H.M.; van Meeteren, L.A.; Houben, A.J.; van Zeijl, L.; Jansen, S. *Nature Structural & Molecular Biology* 2011;18:198.

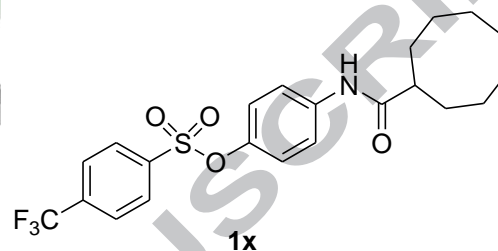
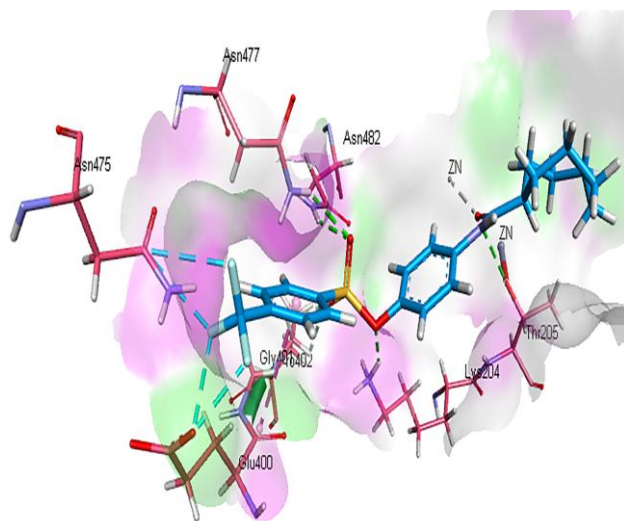
- [30] Addison, W.N.; Azari, F.; Sorensen, E.S.; Kaartinen, M.T.; McKee, M.D. *Journal of Biological Chemistry* 2007;282:15872.
- [31] Buhning, H.J.; Streble, A.; Valent, P. *International Archives of Allergy and Immunology* 2004;133:317.
- [32] Gijsbers, R.; Ceulemans, H.; Stalmans, W.; Bollen, M. *Journal of Biological Chemistry* 2001;276:1361.
- [33] Zalatan, J.G.; Fenn, T.D.; Brunger, A.T.; Herschlag, D. *Biochemistry* 2006;45:9788.
- [34] Scott, L.J.; Delautier, D.; Meerson, N.R.; Trugnan, G.; Goding, J.W.; Maurice, M. *Hepatology* 1997;25:995.
- [35] Stefan, C.; Jansen, S.; Bollen, M. *Purinergic Signalling* 2006;2:361.
- [36] Korekane, H.; Park, J.Y.; Matsumoto, A.; Nakajima, K.; Takamatsu, S.; Ohtsubo, K.; Miyamoto, Y.; Hanashima, S.; Kanekiyo, K.; Kitazume, S.; Yamaguchi, Y. *Journal of Biological Chemistry* 2013;288:27912.
- [37] Johnson, K.; Vaingankar, S.; Chen, Y.; Moffa, A.; Goldring, M.B.; Sano, K.; Jin-Hua, P.; Sali, A.; Goding, J.; Terkeltaub, R. *Arthritis & Rheumatism: Official Journal of the American College of Rheumatology* 1999;42:1986.
- [38] Villa-Bellosta, R.; Wang, X.; Millan, J.L.; Dubyak, G.R.; O'Neill, W.C. *American Journal of Physiology-Heart and Circulatory Physiology* 2011;301:H61.
- [39] Hausmann, J.; Keune, W.J.; Hipgrave Ederveen, A.L.; van Zeijl, L.; Joosten, R.P.; Perrakis, A. *Journal of Structural Biology* 2016;195:199.
- [40] Nishimasu, H.; Okudaira, S.; Hama, K.; Mihara, E.; Dohmae, N.; Inoue, A.; Ishitani, R.; Takagi, J.; Aoki, J.; Nureki, O. *Nature Structural & Molecular Biology* 2011;18:205.
- [41] Jansen, S.; Perrakis, A.; Ulens, C.; Winkler, C.; Andries, M.; Joosten, R.P.; Van Acker, M.; Luyten, F.P.; Moolenaar, W.H.; Bollen, M. *Structure* 2012;20:1948.
- [42] Gorelik, A.; Randriamihaja, A.; Illes, K.; Nagar, B. *The FEBS Journal* 2018;285:2481.
- [43] Iqbal, J.; Lévesque, S.A.; Sévigny, J.; Müller, C.E. *Electrophoresis* 2008; 29:3685.
- [44] Shayhidin, E.; Forcellini, E.; Boulanger, M.C.; Mahmut, A.; Dautrey, S.; Barbeau, X.; Lagüe, P.; Sévigny, J.; Paquin, J.F.; Mathieu, P. *British Journal of Pharmacology* 2015;172:4189.
- [45] Moulharat, N.; Fould, B.; Giganti, A.; Boutin, J.A.; Ferry, G. *Chemico-Biological Interactions* 2008;172:115.

- [46] Parrill, A.L.; Echols, U.; Nguyen, T.; Pham, T.C.T.; Hoeglund, A.; Baker, D.L. *Bioorganic & Medicinal Chemistry* 2008;16:1784.
- [47] Saunders, L.P.; Ouellette, A.; Bandle, R.; Chang, W.C.; Zhou, H.; Misra, R.N.; Enrique, M.; Braddock, D.T. *Molecular Cancer Therapeutics* 2008;7:3352.
- [48] Akhtar, T.; Hameed, S.; Al-Masoudi, N.; Loddo, R.; Colla, P. *Acta Pharmaceutica* 2008;2:135.
- [49] Albers, H.M.; Van Meeteren, L.A.; Egan, D.A.; van Tilburg, E.W.; Moolenaar, W.H.; Ovaa, H. *Journal of Medicinal Chemistry* 2010;53:4958.
- [50] El-Gamal, M.I.; Semreen, M.H.; Foster, P.A.; Potter, B.V.L. *Bioorganic & Medicinal Chemistry* 2016;24:2762.
- [51] Ausekle, E.; Ejaz, S.A.; Khan, S.U.; Ehlers, P.; Villinger, A.; Lecka, J.; Sevigny, J.; Iqbal, J.; Langer, P. *Organic & Biomolecular Chemistry* 2016;14:11402.
- [52] Moulharat, N.; Fould, B.; Giganti, A.; Boutin, J.A.; Ferry, G. *Chemico-Biological Interactions* 2008;172:115.
- [53] Jafari, B.; Yelibayeva, N.; Ospanov, M.; Ejaz, S.A.; Afzal, S.; Khan, S.U.; Abilov, Z.A.; Turmukhanova, M.Z.; Kalugin, S.N.; Safarov, S.; Lecka, J.; Sévigny, J.; Rahman, J.Q.; Ehlers, P.; Iqbal, J.; Langer, P. *RSC Advances* 2016;6:107556.
- [54] Stein, A.J.; Bain, G.; Prodanovich, P.; Santini, A.M.; Darlington, J.; Stelzer, N.M.; Sidhu, R.S.; Schaub; Goulet, L.; Lonergan, D.; Calderon, I.; Evans, J.F.; Hutchinson, J.H. *Molecular Pharmacology* 2015;88:982.
- [55] Gorelik, A.; Randriamihaja, A.; Illes, K.; Nagar, B. *FEBS J* 2018;285:2481.
- [56] MOE (Molecular Operating Environment) Version 2014.0901. Chemical Computing Group, (CCG). http://www.chemcomp.com/MOE_Molecular_Operating_Environment.htm.
- [57] Labute, P. Protonate 3D: Assignment of Macromolecular Protonation State and Geometry, Chemical Computing Group, 2007. <http://www.chemcomp.com/journal/proton.htm>.
- [58] LeadIT version 2.3.2; BioSolveIT GmbH, Sankt Augustin, Germany, 2017, www.biosolveit.de/LeadIT
- [59] Schneider, N.; Lange, G.; Hindle, S.; Klein, R.; Rarey, M. *Journal of Computer-Aided Drug Design* 2013;27:15.

[60] Accelrys Software Inc. Discovery Studio Modeling Environment, Release 4.0; Accelrys Software: San Diego, CA, 2013.

ACCEPTED MANUSCRIPT

Graphical Abstract



IC_{50} (NPP3) = $0.214 \pm 0.012 \mu\text{M}$

Docking pose of compound **1x** into the crystal structure of NPP3